Appendix A.28:

Sabina Playground – VsVp 57192

Table 1: Site Description for Sabina Playground (VsVp 57192).

Attribute	Yes/No			Description/Date	Symbol in Figure 1
	10-m Buffer	20-m Buffer	50-m Buffer		
Near a body of surface water or other free face features?	No	No	No	The center of the site is ~1220 m to the N and ~1750 m to the W from the Avon River; the free face is ~ 1.5-m high. The center of the site is also ~900 m to the W from Horseshoe Lake; the free face is ~ 2.5-m high.	NA
Lateral spreading observed during the CES?	No	No	No	No lateral spreading was observed by the mapping team.[1]	NA
Nearby buildings or structures?	No	Yes	Yes	Building coverage of the 20-m and 50-m buffers is 6% and 17%, respectively. The buildings are in all quadrants of the 50-m buffer and the NW quadrant of the 20-m buffer.	White Fill + Brown Outline
Sloping land?	No	No	No	Flat land, open + residential area	NA
Step changes in the ground surface?	No	No	No	NA	NA
Retaining walls?	No	No	No	NA	NA
Vegetation?	No	Yes	Yes	Trees and bushes cover 5, 4, and 16% of the 10-, 20-, and 50-m buffers, respectively. They are in all quadrants of the 50-m buffer and the NW and NE quadrants of the 20-m buffer.	White Fill + Green Outline
Anthropogenic changes to the site between the LiDAR surveys?	No	No	No	NA	NA
Other important factors?	No	Yes	Yes	Low-motor-vehicle-volume, two-way roadway (Sabina St) occupies 13% of the 20-m buffer and 15% of the 50-m buffer. It stretches throughout the NE and SE quadrants. Playground equipment is in the SW quadrant of the 20-m buffer and the NW and SW quadrants of the 50-m buffer.	Playground Equipment: White Fill +Orange Outline Road: Gray Fill + Red Outline

Note: Buffer is the area within a circle of a specified radius with CPT investigations done at its center (172.660660°, -43.504340°).

[1] Canterbury Geotechnical Database. (2012). "Observed Ground Crack Locations", Map Layer CGD0400 - 23 July 2012, retrieved July 09, 2018 from https://canterburygeotechnicaldatabase.projectorbit.com/

Figure 1: Site plan with areas where ejecta-induced settlement is considered.

Note 1: Patch A (outlined in red) in free field was selected for settlement assessment as an area free of vegetation and structures. Other important factors considered in the selection process were proximity of a patch to a CPT, a property subjected to addition and/or demolition of a structure, front yard/backyard alterations (e.g., ploughing, rubble, scrap), and aerial distribution of sediment ejecta. In addition, the entire portion of the road within the 50-m buffer was considered for settlement assessment. The LiDAR-based settlement analyses were not conducted due to the evident absence of ejecta from Patch A and Road for the Sep-10 EQ, LiDAR flight errors, and misestimation by liquefaction triggering procedures.

Table 2: LiDAR flight error adjustments, global adjustments for the difference between average LiDAR point elevations and benchmark survey elevations, and vertical tectonic movement adjustments.

	Adjustments (mm)		
Earthquake Event(s)	LiDAR Flight Error	Global Offset[2]	Tectonic Vertical Movement
Sep-10	-150	-3	0
Feb-11	+100	16	-75
Jun-11	0	38	-40
Dec-11	0	-65	0
CES	-50	-14	-115
Any LiDAR survey affected by ejecta?			No

Note: The negative sign indicates the subtraction from the ground surface subsidence, while the positive sign indicates the addition to the ground surface subsidence.

Table 3a: LiDAR Measurement Error for Patch A.

Surveys	Buffer	Area Averaged Difference Indicating Repeat Measurement Error (mm)	Ϭ* individual LiDAR points (mm)	%Reduction in Ϭ due to Area Averaging of LiDAR Points
Post Feb 2011: Mar 2011 and May 2011	10-m	ND	59	[ND,ND]
	20-m	ND		
	50-m	ND		
Post Dec 2011: Feb 2012 and Oct 2015	10-m	ND	70	[ND,ND]
	20-m	ND		
	50-m	ND		

*Standard deviation; ND = Not determined.

[2] Russell, J., & van Ballegooy, S. (2015). *Canterbury Earthquake Sequence: Increased liquefaction vulnerability assessment methodology*. New Zealand: Tonkin & Taylor Ltd.

Table 3b: LiDAR Measurement Error for Road.

Surveys	Buffer	Area Averaged Difference Indicating Repeat Measurement Error (mm)	$\sigma^*_{\text{individual LiDAR points}}$ (mm)	%Reduction in σ due to Area Averaging of LiDAR Points
Post Feb 2011: Mar 2011 and May 2011	10-m	NA	59	[ND,ND]
	20-m	ND		
	50-m	ND		
Post Dec 2011: Feb 2012 and Oct 2015	10-m	NA	70	[ND,ND]
	20-m	ND		
	50-m	ND		

*Standard deviation; NA = Not available; ND = Not determined.

Table 4a: Ground surface subsidence adjustments due to LiDAR measurement error for Patch A.

Earthquake Event(s)	$\sigma_{\text{pre-EQ LiDAR survey}}$ (mm)	$\sigma_{\text{post-EQ LiDAR survey}}$ (mm)	σ_{total} (mm)	Area Average Adjusted σ (mm) **
Sep-10	158	56	134	ND
Feb-11	56	59	59	ND
Jun-11	59	61	62	ND
Dec-11	61	70	87	ND
CES	158	70	124	ND

**Based on the highest %Reduction in Table 3a.

Table 4b: Ground surface subsidence adjustments due to LiDAR measurement error for Road

Earthquake Event(s)	$\sigma_{\text{pre-EQ LiDAR survey}}$ (mm)	$\sigma_{\text{post-EQ LiDAR survey}}$ (mm)	σ_{total} (mm)	Area Average Adjusted σ (mm) **
Sep-10	158	56	134	ND
Feb-11	56	59	59	ND
Jun-11	59	61	62	ND
Dec-11	61	70	87	ND
CES	158	70	124	ND

**Based on the highest %Reduction in Table 3b.

Table 5a: Raw liquefaction-related ground surface subsidence using original LiDAR points for Patch A.

Earthquake Event(s)	Average Ground Surface Subsidence (mm)		
	10-m Buffer	20-m Buffer	50-m Buffer
Sep-10	ND	ND	ND
Feb-11	ND	ND	ND
Jun-11	ND	ND	ND
Dec-11	ND	ND	ND
CES	ND	ND	ND

ND = Not determined.

Table 5b: Raw liquefaction-related ground surface subsidence using original LiDAR points for Road.

Earthquake Event(s)	Average Ground Surface Subsidence (mm)		
	10-m Buffer	20-m Buffer	50-m Buffer
Sep-10	NA	ND	ND
Feb-11	NA	ND	ND
Jun-11	NA	ND	ND
Dec-11	NA	ND	ND
CES	NA	ND	ND

ND = Not determined; NA = Not available.

Table 6a: Corrected liquefaction-related ground surface subsidence using original LiDAR points for Patch A with the calculated adjustments in Table 2.

Earthquake Event(s)	Average Calculated Ground Surface Subsidence (mm)		
	10-m Buffer	20-m Buffer	50-m Buffer
Sep-10	ND	ND	ND
Feb-11	ND	ND	ND
Jun-11	ND	ND	ND
Dec-11	ND	ND	ND
CES	ND	ND	ND

Notes: Plus/minus values are same as those in Table 4a, but rounded to the nearest 25; Positive overall values indicate ground surface subsidence, while negative overall values indicate ground surface uplift.

Table 6b: Corrected liquefaction-related ground surface subsidence using original LiDAR points for Road with the calculated adjustments in Table 2.

	Average Calculated Ground Surface Subsidence (mm)		
Earthquake Event(s)	10-m Buffer	20-m Buffer	50-m Buffer
Sep-10	NA	ND	ND
Feb-11	NA	ND	ND
Jun-11	NA	ND	ND
Dec-11	NA	ND	ND
CES	NA	ND	ND

Notes: Plus/minus values are same as those in Table 4b, but rounded to the nearest 25; Positive overall values indicate ground surface subsidence, while negative overall values indicate ground surface uplift.

Table 7a: Corrected liquefaction-related ground surface subsidence for Patch A using LiDAR DEMs.

	Estimated Ground Surface Subsidence (mm)								
	10-m Buffer			20-m Buffer			50-m Buffer		
Earthquake Event(s)	16th %ile	50th %ile	84th %ile	16th %ile	50th %ile	84th %ile	16th %ile	50th %ile	84th %ile
Sep-10	<50	<50	<50	<50	<50	<50	<50	<50	<50
Feb-11	100	150	150	100	150	150	100	150	150
Jun-11	<50	50	50	<50	50	50	<50	50	50
Dec-11	<50	50	50	<50	50	50	<50	50	50
CES	100	200	200	100	200	200	100	200	200

Note: These percentiles are not the exact statistical measures; they indicate the spatial variability of ground surface subsidence.

Table 7b: Corrected liquefaction-related ground surface subsidence for Road using LiDAR DEMs.

	Estimated Ground Surface Subsidence (mm)								
	10-m Buffer			20-m Buffer			50-m Buffer		
Earthquake Event(s)	16th %ile	50th %ile	84th %ile	16th %ile	50th %ile	84th %ile	16th %ile	50th %ile	84th %ile
Sep-10	NA	NA	NA	<50	<50	<50	<50	<50	50
Feb-11	NA	NA	NA	100	150	150	100	150	150
Jun-11	NA	NA	NA	<50	50	50	<50	50	50
Dec-11	NA	NA	NA	<50	50	50	<50	50	50
CES	NA	NA	NA	150	200	200	150	200	200

Note: These percentiles are not the exact statistical measures; they indicate the spatial variability of ground surface subsidence.

Table 8a: Ejecta-Induced settlement for the top 20 m of the soil profile for Patch A (10-, 20-, and 50-m buffers) for the 50th %ile PGA, P_L=50%, and C_{FC}=0.13 using BI-2014, ZRB-2002, and I_C cutoff of 2.6.

Earthquake Event(s)	M_W	PGA (g)	Depth to Groundwater (m)	S_T (mm)	S_{V1D} (mm)	$S_{E,L}$ (mm)
Sep-10	7.1	0.19	1.8	ND	0 ± 20	ND
Feb-11	6.2	0.35	1.7	ND	3 ± 50	ND
Jun-11	6.2	0.20	1.3	ND	0 ± 25	ND
Dec-11	6.1	0.27	1.0	ND	1 ± 50	ND

Notes: S_T = Total settlement (Table 6); S_{V1D} = Average vertical settlement due to volumetric compression using Boulanger and Idriss (2014) (BI-2014), Zhang et al. (2002) (ZRB-2002) procedures and de Greef and Lengkeek (2018) thin-layer correction; $S_{E,L}$ = Ejecta-induced settlement as the difference between the LiDAR-based S_T and S_{V1D}.

Table 8d: Ejecta-Induced settlement for the top 20 m of the soil profile for Road within the 50-m buffer for the 50th %ile PGA, P_L=50%, and C_{FC}=0.13 using BI-2014, ZRB-2002, and I_C cutoff of 2.6.

Earthquake Event(s)	M_W	PGA (g)	Depth to Groundwater (m)	S_T (mm)	S_{V1D} (mm)	$S_{E,L}$ (mm)
Sep-10	7.1	0.19	1.8	ND	2 ± 20	ND
Feb-11	6.2	0.35	1.7	ND	7 ± 50	ND
Jun-11	6.2	0.20	1.3	ND	2 ± 25	ND
Dec-11	6.1	0.27	1.0	ND	5 ± 50	ND

Notes: S_T = Total settlement (Table 6); S_{V1D} = Average vertical settlement due to volumetric compression using Boulanger and Idriss (2014) (BI-2014), Zhang et al. (2002) (ZRB-2002) procedures and de Greef and Lengkeek (2018) thin-layer correction; $S_{E,L}$ = Ejecta-induced settlement as the difference between the LiDAR-based S_T and S_{V1D}.

Note 2: The uncertainty for volumetric settlement was derived based on the sensitivity of volumetric settlement to PGA, C_{FC}, and P_L for each earthquake event for VsVp 57203 *Shirley Intermediate School* and CC LIQ 1 – CPT 5586 – *Vivian St* sites. Taking the 50th percentile as the baseline case, the minimum and maximum values corresponding to the difference between the 25th percentile and the 50th percentile and the 75th percentile and the 50th percentile were determined. The arithmetic mean of the range of the minimum and maximum difference was evaluated for each patch at the two sites. The maximum arithmetic mean for each earthquake event was rounded to the nearest five and used as the uncertainty value. Accordingly, the 1-D volumetric settlement uncertainties of ± 20, ± 50, ± 25, and ± 50 mm for the Sep-10, Feb-11, Jun-11, and Dec-11 earthquake events, respectively, were used for all sites in this study.

Table 9a: Coverage area and height of ejecta estimates for Patch A (10-m buffer) using photographs.

EQ Event	$H_{E,thick}$ (mm)	$A_{E,thick}$ (m^2)	$H_{E,thin}$ (mm)	$A_{E,thin}$ (m^2)	A_T (m^2)
Sep-10	0	0	0	0	296
Feb-11	60-100	27.1	10-20	114	296
Jun-11	0	0	20-30	192	296
Dec-11	0	0	10-20	3.9	288

Notes: $A_{E,thin/thick}$ = Coverage area of thin/thick ejecta layers; $H_{E, thin/thick}$ = Lower-upper estimate of height of thin/thick ejecta layers; A_T= Total assessment area of a buffer being considered.

Table 9b: Coverage area and height of ejecta estimates for Patch A (20-m buffer) using photographs.

EQ Event	$H_{E,thick}$ (mm)	$A_{E,thick}$ (m^2)	$H_{E,thin1}$ (mm)	$A_{E,thin1}$ (m^2)	$H_{E,thin2}$ (mm)	$A_{E,thin2}$ (m^2)	A_T (m^2)
Sep-10	0	0	0	0	0	0	710
Feb-11	100-180	23.9	60-100	27.1	10-20	178	710
Jun-11	0	0	0	0	20-30	342	710
Dec-11	0	0	30-60	1.6	10-20	10.0	701

Notes: $A_{E,thin/thick}$ = Coverage area of thin/thick ejecta layers; $H_{E, thin/thick}$ = Lower-upper estimate of height of thin/thick ejecta layers; A_T= Total assessment area of a buffer being considered.

Table 9c: Coverage area and height of ejecta estimates for Patch A (50-m buffer) using photographs.

EQ Event	$H_{E,thick}$ (mm)	$A_{E,thick}$ (m^2)	$H_{E,thin1}$ (mm)	$A_{E,thin1}$ (m^2)	$H_{E,thin2}$ (mm)	$A_{E,thin2}$ (m^2)	A_T (m^2)
Sep-10	0	0	0	0	0	0	885
Feb-11	100-180	79.4	60-100	27.1	10-20	233	885
Jun-11	0	0	0	0	20-30	347	885
Dec-11	0	0	30-60	10.2	10-20	13.3	860

Notes: $A_{E,thin/thick}$ = Coverage area of thin/thick ejecta layers; $H_{E, thin/thick}$ = Lower-upper estimate of height of thin/thick ejecta layers; A_T= Total assessment area of a buffer being considered.

Table 9d: Coverage area and height of ejecta estimates for Road (50-m buffer) using photographs.

EQ Event	$H_{E,prism/pyr}$ (mm)	$V_{E,prism+pyr}$ (m³)	$H_{E,thin}$ (mm)	$A_{E,thin}$ (m²)	$H_{E,thick}$ (mm)	$A_{E,thick}$ (m²)	A_T (m²)
Sep-10	0	0	0	0	0	0	1297
Feb-11	19-300	49.9-81.3	2-4	530	0	0	1297
Jun-11	26-266	26.4-48.4	2-3	658	0	0	1225
Dec-11	15-200	2.7-3.3	5-10	9.1	10-20	74.7	1282

Notes: $H_{E,prism/pyr}$ = Lower-upper estimate of ejecta height near the curb based on 2-4% cross slope of normal crown; $V_{E,prism+pyr}$ = Lower-upper estimate of total volume of prismatic- and pyramidal-shape ejecta; $A_{E,thin/thick}$ =Coverage area of thin/thick ejecta layers; $H_{E,\ thin/thick}$ = Lower-upper estimate of height of thin/thick ejecta layers; A_T= Total assessment area of a buffer being considered.

Note 3: The values in Table 9 correspond to the coverage area of ejecta outlined in aerial photographs (Figures 35-37) and the lower and upper estimates of ejecta height based on geometrical approximations, ground photographs (Figure 38), and EQC LDAT property inspection reports. The ejecta-induced settlement using photographs and engineering judgment, $S_{E,P}$, is estimated as

$$S_{E,P} = \frac{\sum_{i=1}^{a} A_{E,thick,i} * H_{E,thick,i} + \sum_{j=1}^{b} A_{E,thin,j} * H_{E,thin,j}}{A_T} + \frac{\frac{1}{2}\sum_{n=1}^{f} W_{E,prism,n} * H_{E,prism,n} * L_{E,prism,n}}{A_T} + \frac{\frac{1}{3}\sum_{p=1}^{g} W_{E,pyramid1,p} * H_{E,pyramid1,p} * L_{E,pyramid1,p}}{A_T} + \frac{\frac{1}{6}\sum_{r=1}^{h} W_{E,pyramid2,r} * H_{E,pyramid2,r} * L_{E,pyramid2,r}}{A_T}$$

$$= \frac{\sum_{i=1}^{a} V_{E,thick,i} + \sum_{j=1}^{b} V_{E,thin,j} + \sum_{n=1}^{f} V_{E,prism,n} + \sum_{p=1}^{g} V_{E,pyramid,p}}{A_T} + \frac{\sum_{r=1}^{h} V_{E,pyramid2,p}}{A_T}$$

where

- $A_{E,thick,i}$ and $H_{E,thick,i}$ are the area and the height of a thick ejecta layer, respectively;
- $A_{E,thin,j}$ and $H_{E,thin,j}$ are the area and the height of a thin ejecta layer, respectively;
- $W_{E,prism,n}$ and $L_{E,prism,n}$ are the width and the length of the coverage area of a prismatically shaped ejecta layer, respectively, and $H_{E,prism,n}$ is the height of a prism-like ejecta layer;
- $W_{E,pyramid1,p}$ and $L_{E,pyramid1,p}$ are the width and the length of the coverage area of a pyramid-like rectangular-base ejecta layer, respectively, and $H_{E,pyr,p}$ is the height of a pyramid-like rectangular-base ejecta layer;
- $W_{E,pyramid2,r}$ and $L_{E,pyramid2,r}$ are the width and the length of the coverage area of a pyramid-like triangular-base ejecta layer, respectively, and $H_{E,pyr,p}$ is the height of a pyramid-like triangular-base ejecta layer;

- A_T is the total assessment area for a buffer being considered (Figure 1).

Table 10a: Ejecta-induced settlement estimates for Patch A based on photographs.

Earthquake Event	Patch A (10-m buffer)		Patch A (20-m buffer)		Patch A (50-m buffer)	
	$S_{E,P,lower}$ (mm)	$S_{E,P,upper}$ (mm)	$S_{E,P,lower}$ (mm)	$S_{E,P,upper}$ (mm)	$S_{E,P,lower}$ (mm)	$S_{E,P,upper}$ (mm)
Sep-10	0	0	0	0	0	0
Feb-11	9	17	8	15	13	25
Jun-11	13	20	10	15	8	12
Dec-11	≈0	≈0	≈0	≈0	≈0	1

Note: $S_{E,P,lower}$ and $S_{E,P,upper}$ correspond to lower and upper estimates of $S_{E,P}$, respectively.

Table 10b: Ejecta-induced settlement estimates for Road based on photographs.

Earthquake Event	Road (50-m buffer)	
	$S_{E,P,lower}$ (mm)	$S_{E,P,upper}$ (mm)
Sep-10	0	0
Feb-11	39	64
Jun-11	23	41
Dec-11	3	4

Note: $S_{E,P,lower}$ and $S_{E,P,upper}$ correspond to lower and upper estimates of $S_{E,P}$, respectively.

Table 11a: Best final estimates of ejecta-induced settlement for Patches A, B, and C.

EQ Event	Patch A (10-m buffer)			Patch A (20-m buffer)			Patch A (50-m buffer)		
	$S_{E,L}$ (mm)	$S_{E,P}$ (mm)	$S_{E,final}$ (mm)	$S_{E,L}$ (mm)	$S_{E,P}$ (mm)	$S_{E,final}$ (mm)	$S_{E,L}$ (mm)	$S_{E,P}$ (mm)	$S_{E,final}$ (mm)
Sep-10	ND	0	0	ND	0	0	ND	0	0
Feb-11	ND	13±4	15±5	ND	11.5±3.5	10±5	ND	19±6	20±5
Jun-11	ND	16.5±3.5	15±5	ND	12.5±2.5	15±5	ND	10±2	10±5
Dec-11	ND	≈0	<5	ND	≈0	<5	ND	0.5±0.5	<5

Notes: $S_{E,L}$ = Ejecta-induced settlement based on LiDAR data reported in Table 8; $S_{E,P}$ = Median ejecta-induced settlement for the range of values reported in Table 10; $S_{E,final}$ = Best final estimate of ejecta-induced settlement rounded to the nearest 5; Final plus/minus values are also rounded to the nearest 5; ND = Not determined.

Table 11b: Best final estimates of ejecta-induced settlement for Road (20-m and 50-m buffers).

Earthquake Event	Road (50-m buffer)		
	$S_{E,L}$ (mm)	$S_{E,P}$ (mm)	$S_{E,final}$ (mm)
Sep-10	ND	0	0
Feb-11	ND	52±12	50±10
Jun-11	ND	32±9	30±10
Dec-11	ND	3.5±0.5	5±5

Notes: $S_{E,L}$ = Ejecta-induced settlement based on LiDAR data reported in Table 8; $S_{E,P}$ = Median ejecta-induced settlement for the range of values reported in Table 10; $S_{E,final}$ = Best final estimate of ejecta-induced settlement rounded to the nearest 5; Final plus/minus values are also rounded to the nearest 5; ND = Not determined.

Note 4:

- $S_{E,final}$ is based solely on $S_{E,P}$ for all earthquake events.
- The Sabina Playground site is in the apparent zone of higher ground surface subsidence for the Sep-10 EQ (i.e., the overestimate of the ground surface elevation by the Jul-03 LiDAR survey and the underestimate of the ground surface elevation by the Sep-10 LiDAR survey) and the apparent zone of lower ground surface subsidence for the Feb-11 EQ (i.e., the underestimate of the ground surface elevation by the Sep-10 LiDAR survey). The site is also in the zone of accurate LPI prediction of liquefaction severity for the Sep-10 and slight to moderate LPI underprediction of liquefaction severity for the Feb-11 EQ (Maurer et al. 2014[3]). The LDAT property inspection reports from May 2011 are available for properties within the 50-m buffer. There are ground photographs that show ejecta remnants at these properties. No ground photographs of Patch A and Road were acquired.

<u>Summary 1</u>:

- **The best estimate of the ejecta-induced free-field ground settlement at the Sabina Playground site for the SEP 2010, FEB 2011, JUN 2011, and DEC 2011 earthquake is 0 mm, 20±5 mm, 10±5 mm, and <5 mm, respectively.**
- **The best estimate of the ejecta-induced free-field ground settlement of the road at the Sabina Playground site for the SEP 2010, FEB 2011, JUN 2011, and DEC 2011 earthquake is 0 mm, 50±10 mm, 30±10 mm, and 5±5 mm, respectively.**

[3] Maurer, B. W., Green, R. A., Cubrinovski, M., & Bradley, B. A. (2014). Evaluation of the Liquefaction Potential Index for Assessing Liquefaction Hazard in Christchurch, New Zealand. *Journal of Geotechnical and Geoenvironmental Engineering*, 140(7), 04014032-1-11. doi:10.1061/(asce)gt.1943-5606.0001117

Figure 2: Location of the site.

Figure 3: Position of the site relative to nearby free-face features.

Figure 4: Position of the site relative to nearby buildings and vegetation.

Figure 5: Street view of the flat land.

Figure 6: Satellite image of the site taken in Dec 2004.

Figure 7: Satellite image of the site taken in Mar 2009.

Figure 8: Satellite image of the site taken on Sep 3, 2010.

Figure 9: Satellite image of the site taken on Sep 5, 2010.

Figure 10: Satellite image of the site taken on Feb 7, 2011.

Figure 14: Satellite image of the site taken on Feb 26, 2011.

Figure 12: Satellite image of the site taken on Mar 28, 2011.

Figure 13: Satellite image of the site taken in Apr 2012.

Figure 14: Satellite image of the site taken in Nov 2015.

Figure 15: Aerial photograph of the site taken on Sep 4, 2010.

Figure 16: Aerial photograph of the site taken on Feb 24, 2011.

Figure 17: Aerial photograph of the site taken on June 14-15, 2011.

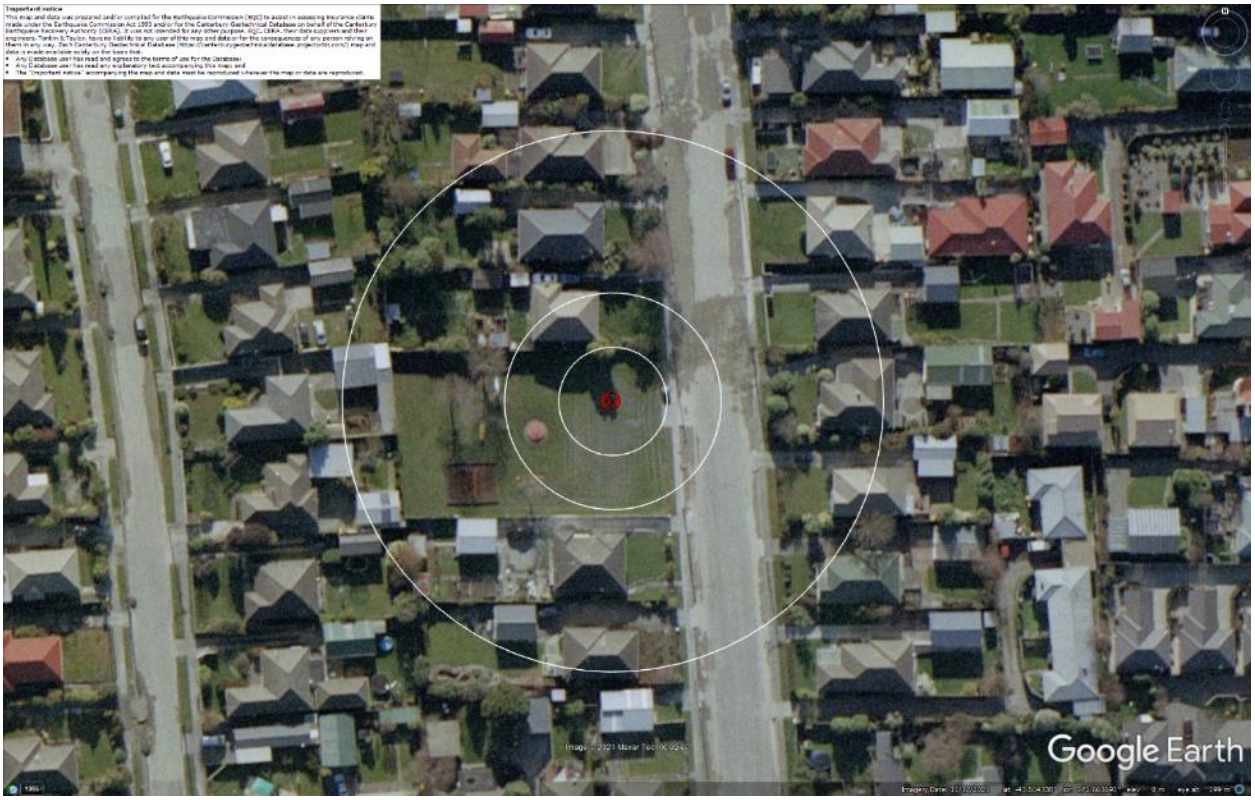

Figure 18: Aerial photograph of the site taken on June 16, 2011.

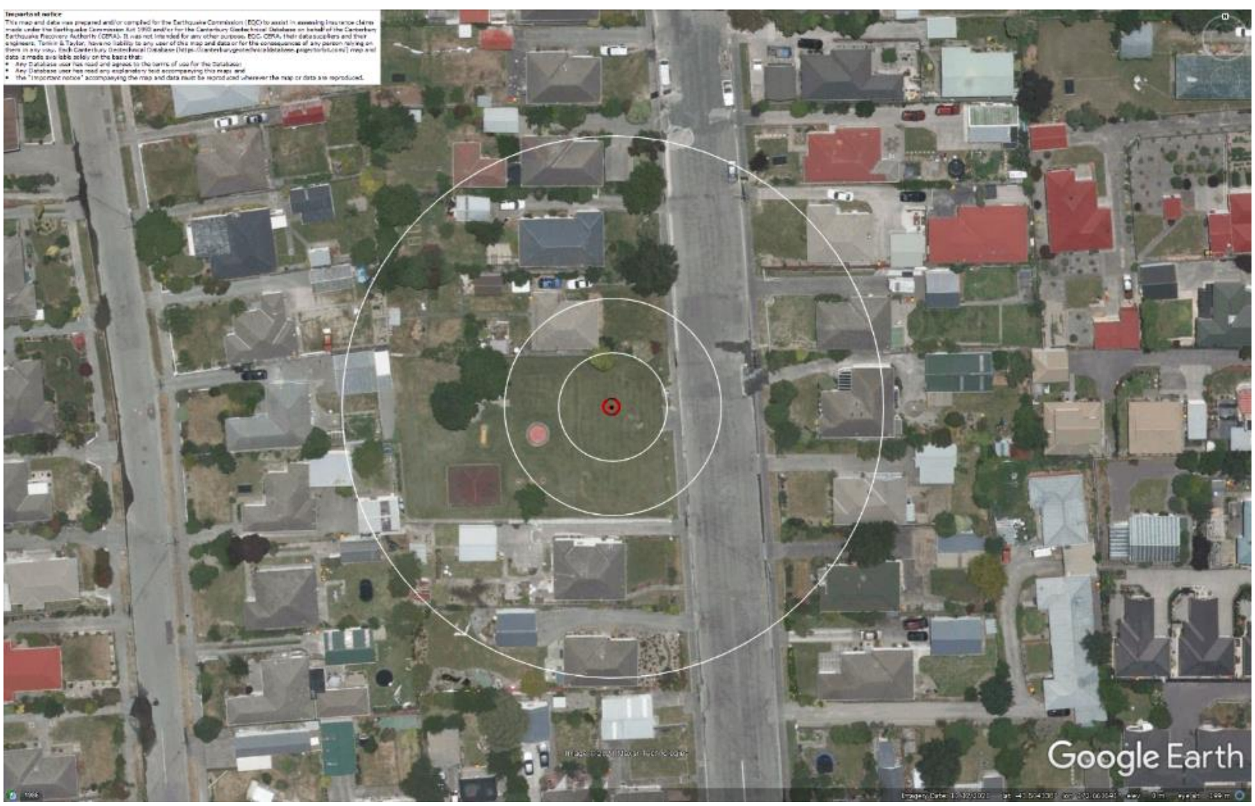

Figure 19: Aerial photograph of the site taken on Dec 24, 2011.

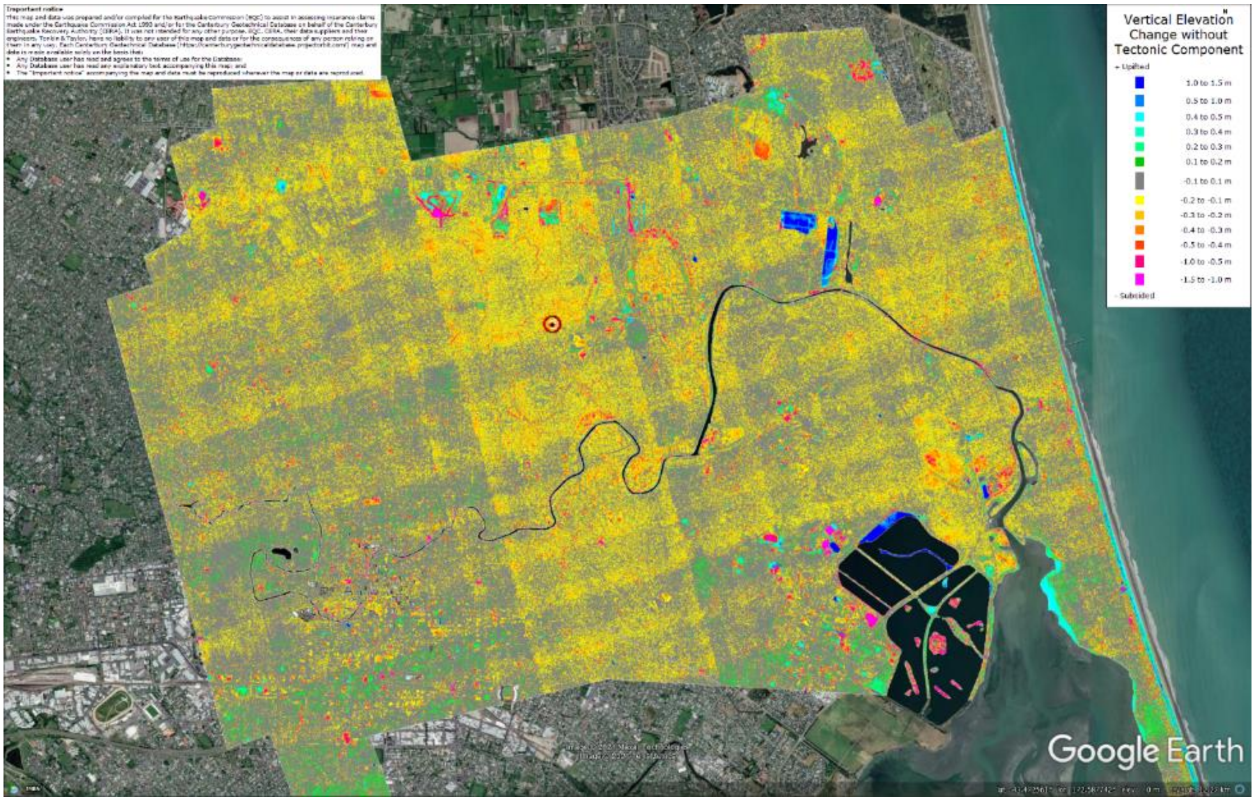

Figure 20: Vertical Ground Movements (Surface – Tectonic) for Sep 2010 Earthquake – the site is in the apparent zone of overestimated ground surface subsidence (i.e., flight error bands for July 2003 and Sep 2010).

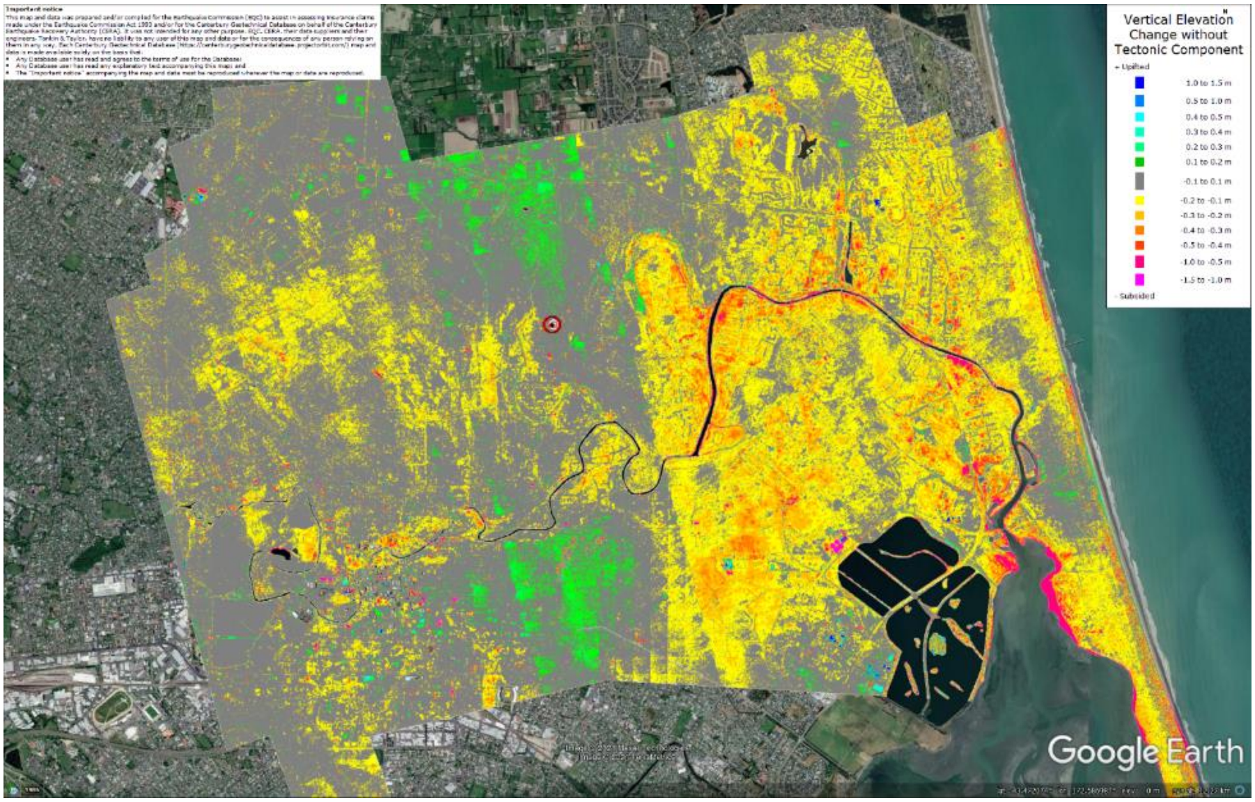

Figure 21: Vertical Ground Movements (Surface – Tectonic) for Feb 2011 Earthquake – the site is in the apparent zone of underestimated ground surface subsidence (i.e., flight error band for Sep 2010).

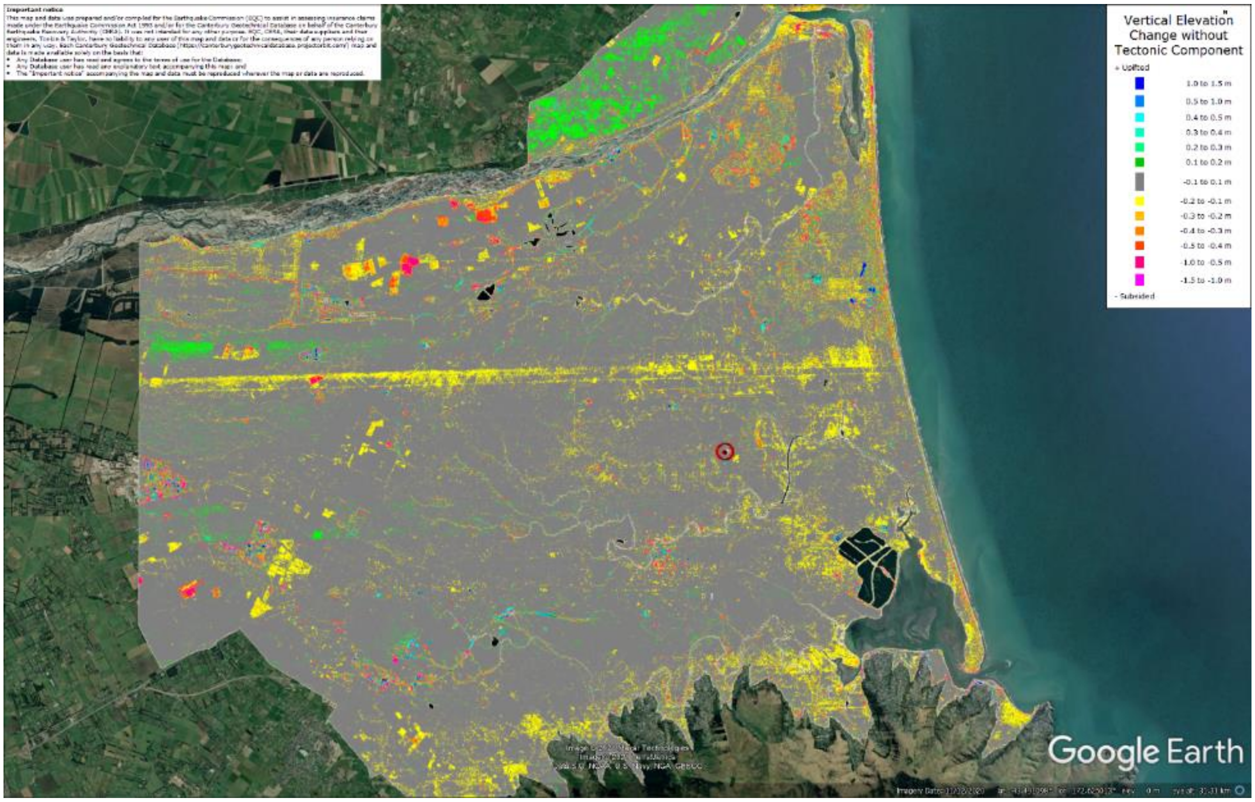

Figure 22: Vertical Ground Movements (Surface – Tectonic) for June 2011 Earthquake – the site is not in the apparent zone of overestimated or underestimated ground surface subsidence.

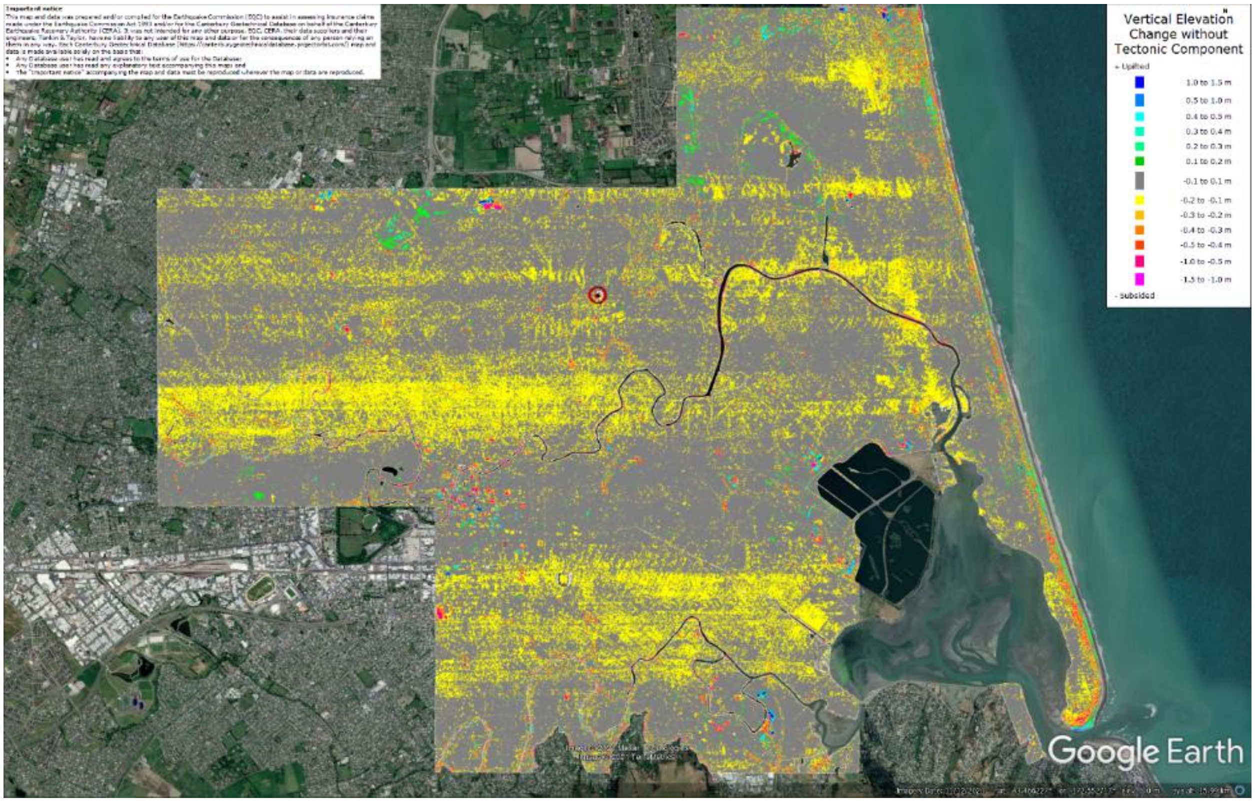

Figure 23: Vertical Ground Movements (Surface – Tectonic) for Dec 2011 Earthquake – the site is not in the apparent zone of overestimated or underestimated ground surface subsidence.

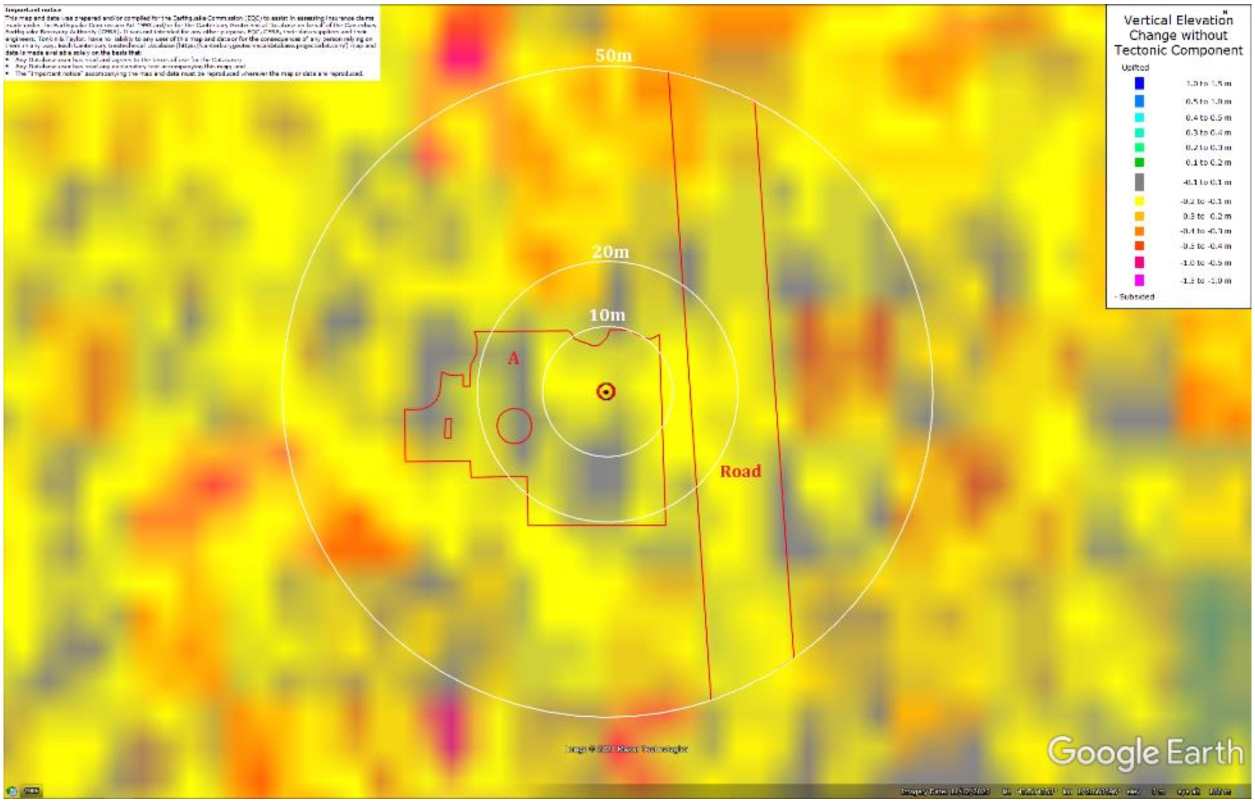

Figure 24: Ground surface subsidence without tectonic component for Sep 2010 Earthquake according to the LiDAR DEM.

Figure 25: Ground surface subsidence without tectonic component for Feb 2011 Earthquake according to the LiDAR DEM.

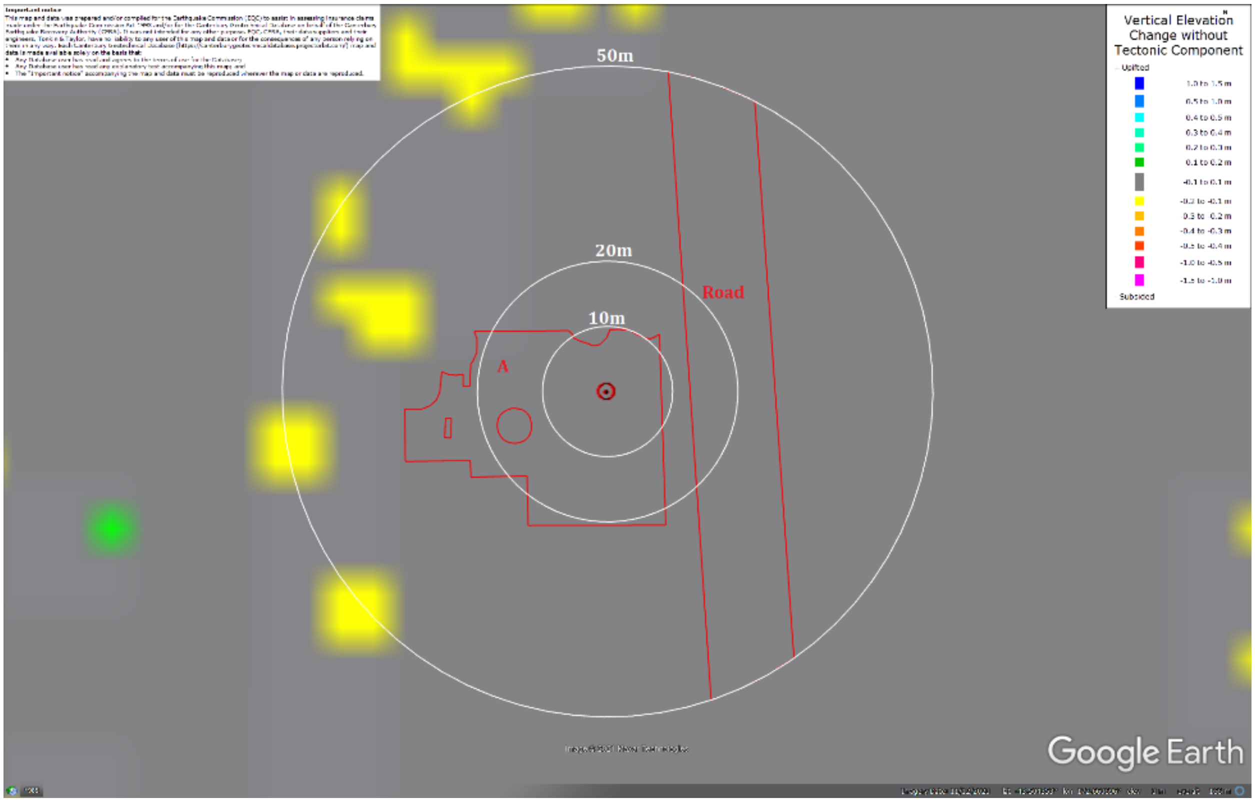

Figure 26: Ground surface subsidence without tectonic component for June 2011 Earthquake according to the LiDAR DEM.

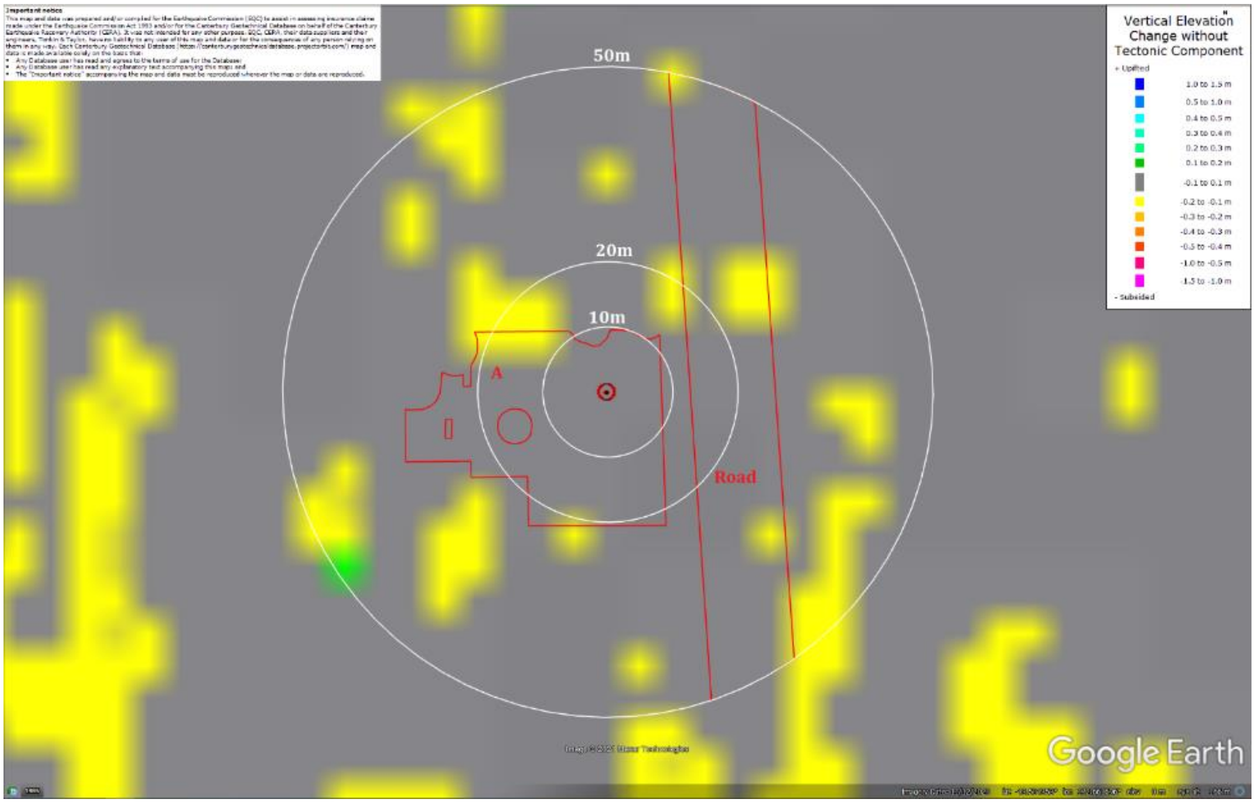

Figure 27: Ground surface subsidence without tectonic component for Dec 2011 Earthquake according to the LiDAR DEM.

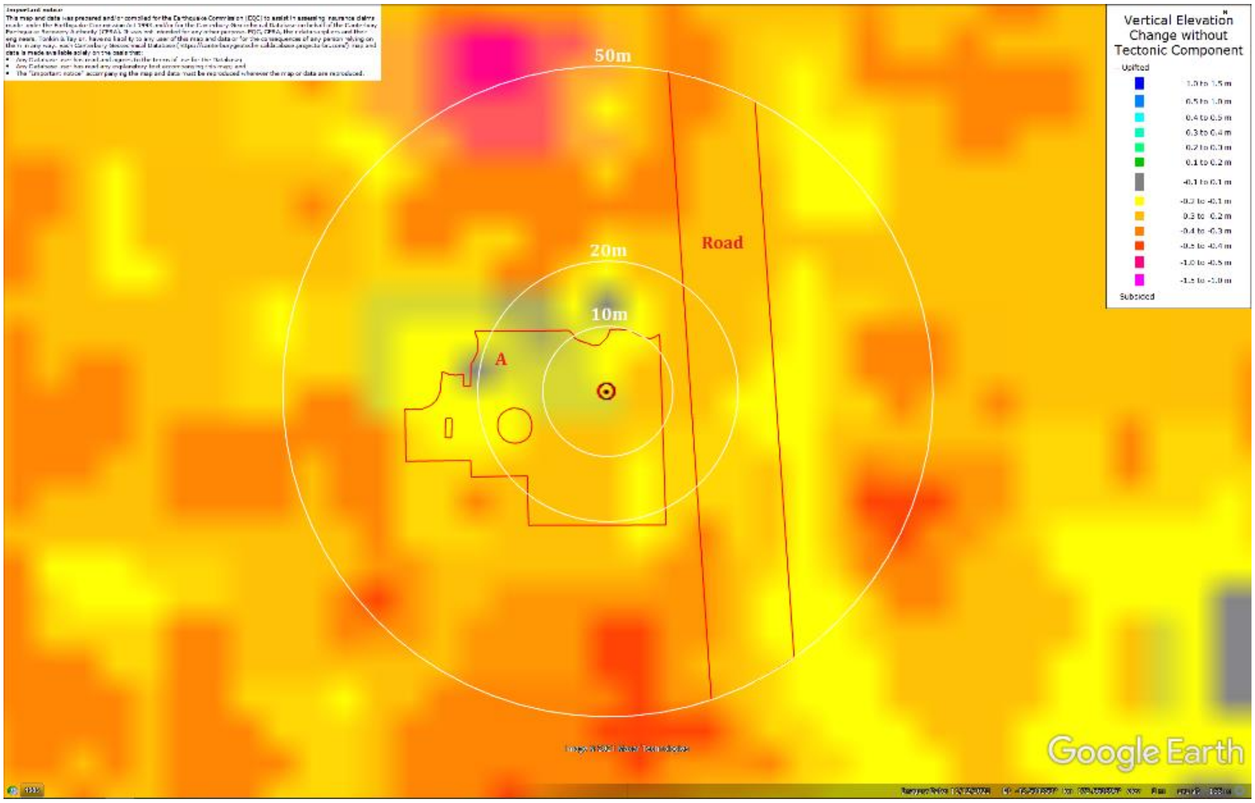

Figure 28: Ground surface subsidence without tectonic component for Canterbury Earthquake Sequence according to the LiDAR DEM.

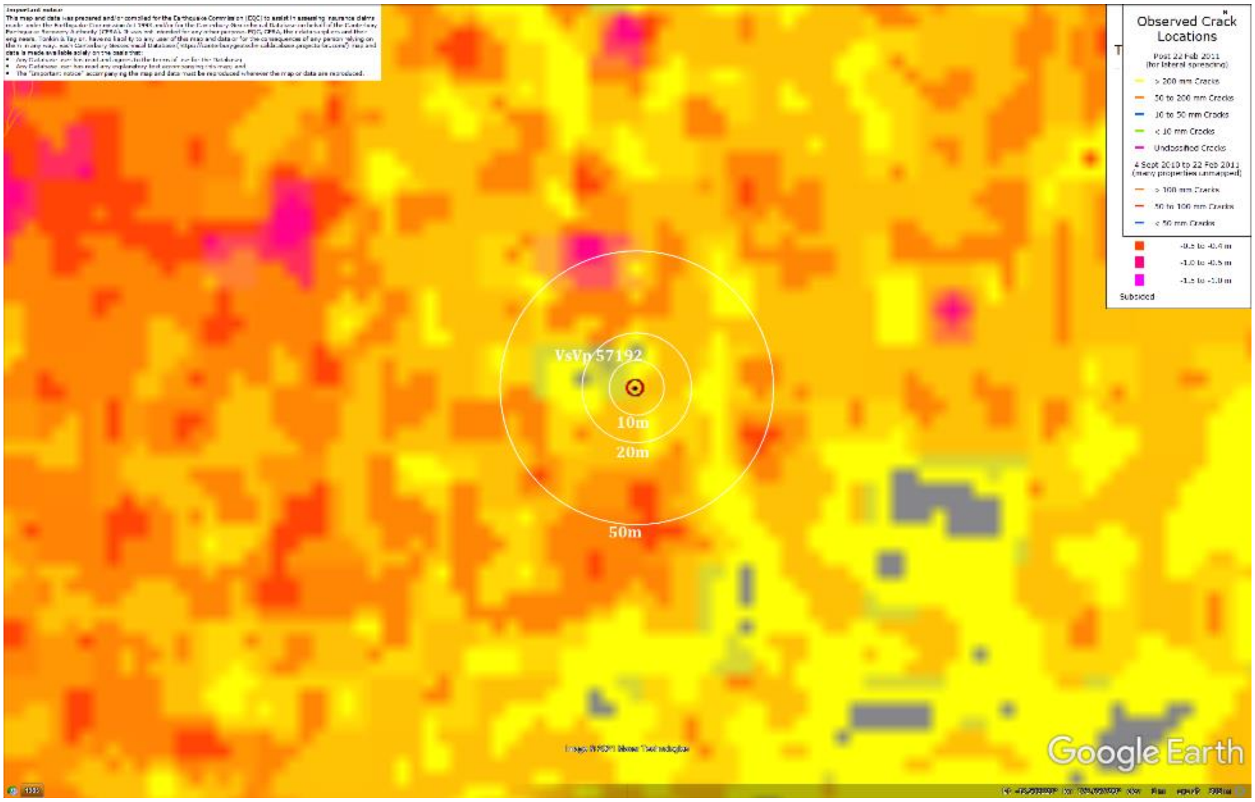

Figure 29: No lateral spreading for Canterbury Earthquake Sequence.

Figure 30: Vertical tectonic movements for Sep 2010 Earthquake.

Figure 31: Vertical tectonic movements for Feb 2011 Earthquake.

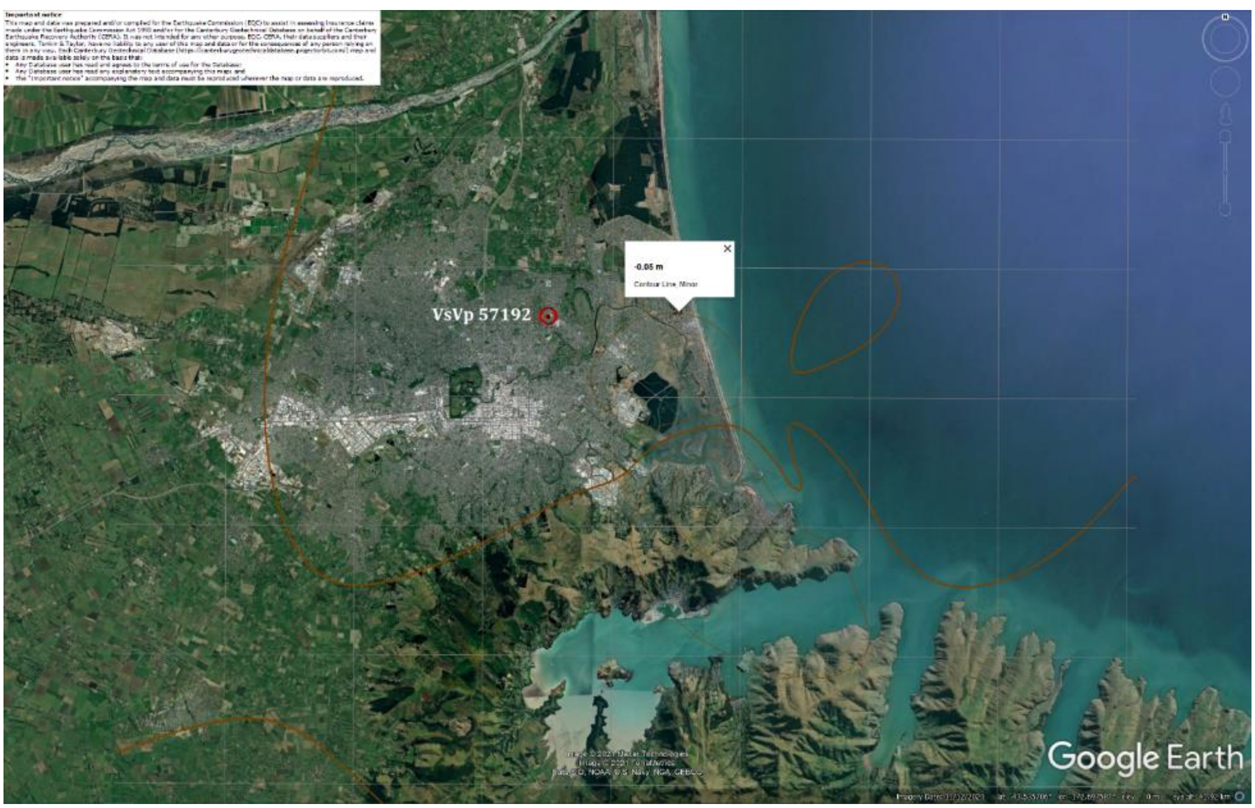

Figure 32: Vertical tectonic movements for June 2011 Earthquake.

Figure 33: Vertical tectonic movements for Dec 2011 Earthquake.

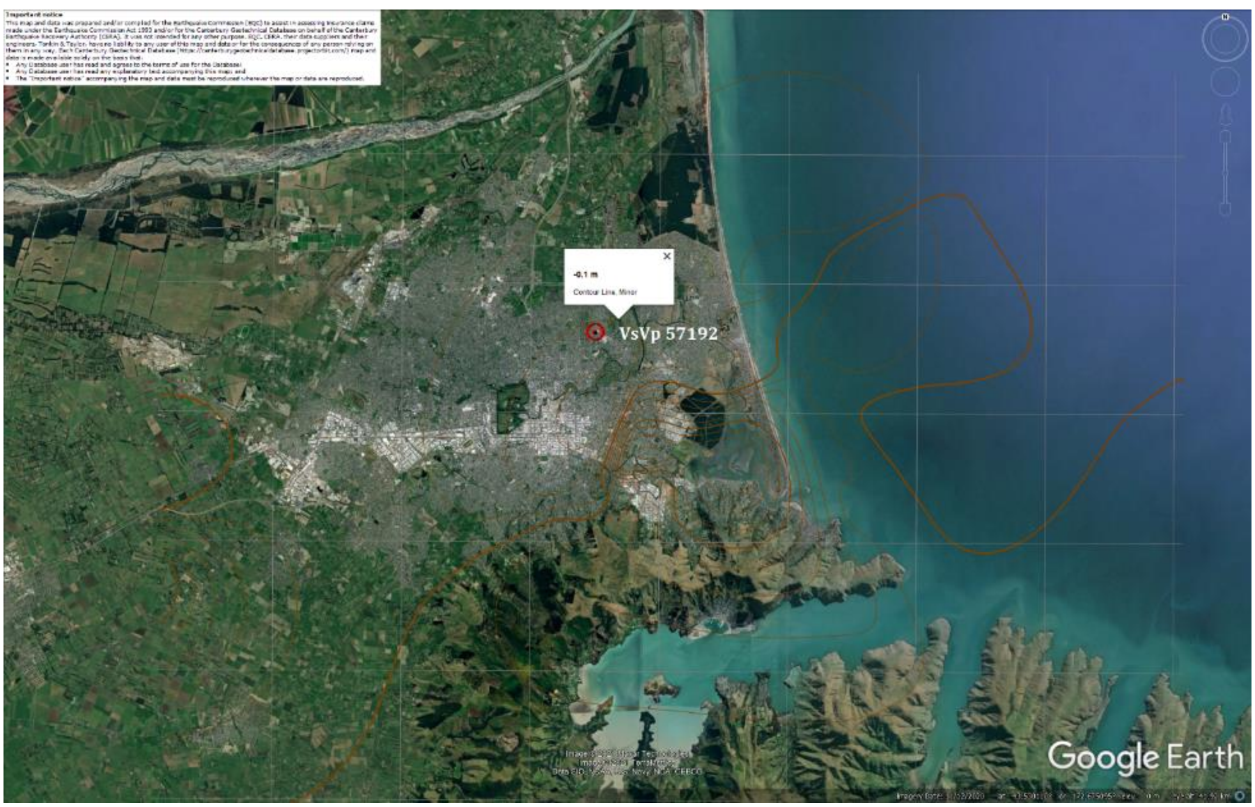

Figure 34: Vertical tectonic movements for Canterbury Earthquake Sequence.

Figure 35: Aerial photograph showing the ejecta outline at the site for Feb-11 EQ.

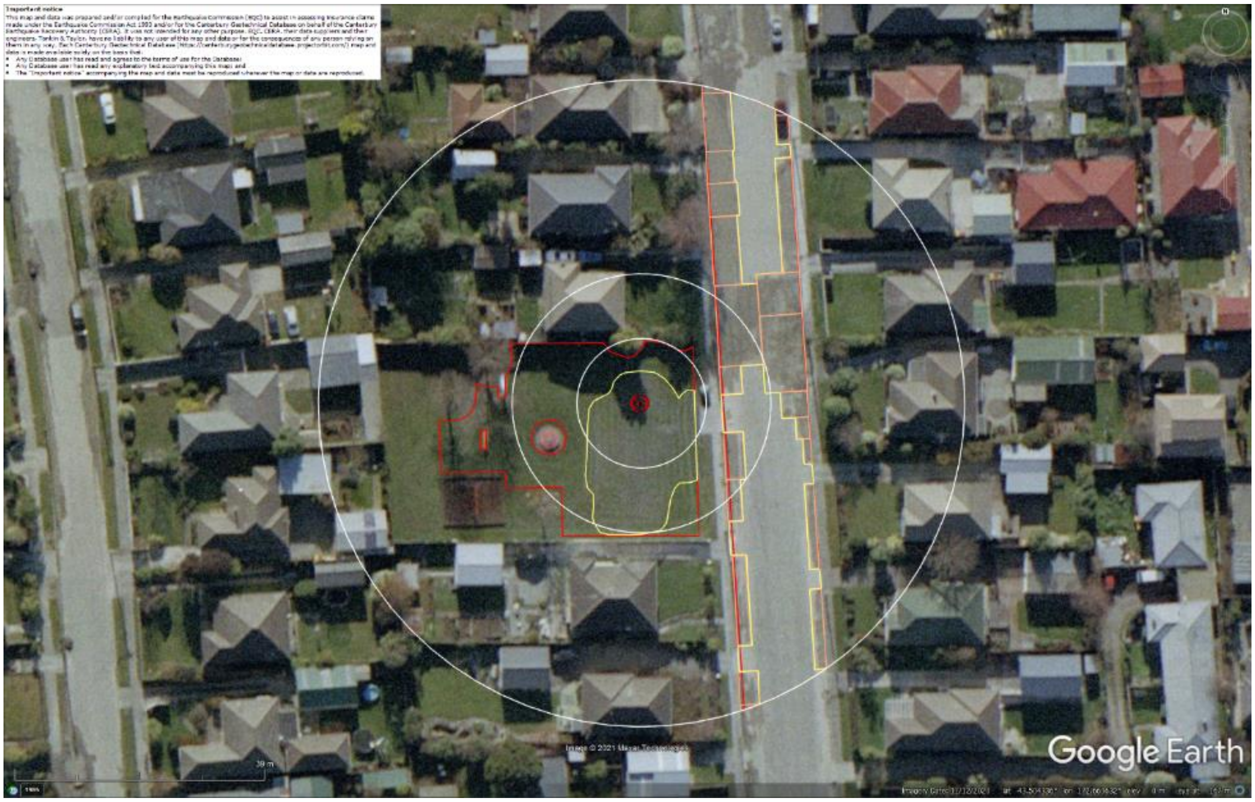

Figure 36: Aerial photograph acquired on 16 Jun 2011 showing the ejecta outline at the site for Jun-11 EQ.

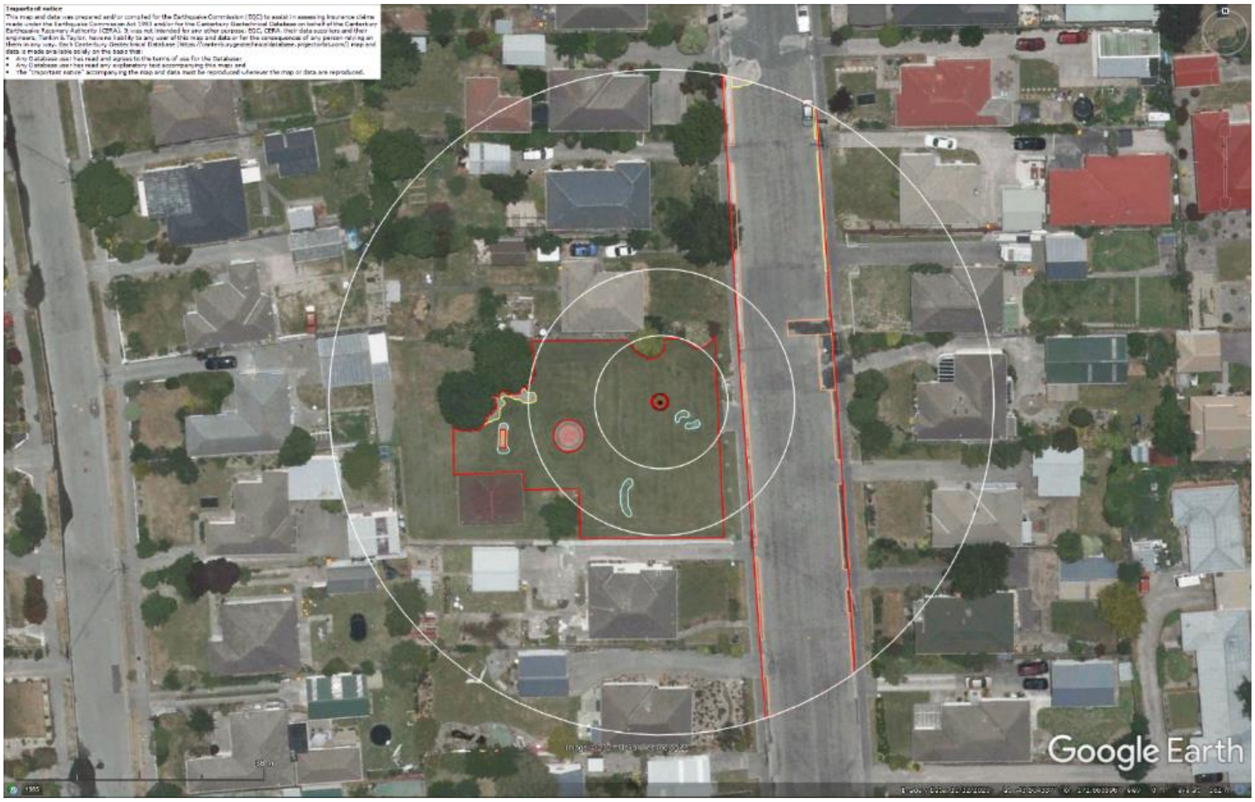

Figure 37: Aerial photograph showing the ejecta outline at the site for Dec-11 EQ.

Figure 38: Ground photographs showing ejecta remnants at nearby properties (photograph date: May 2011).

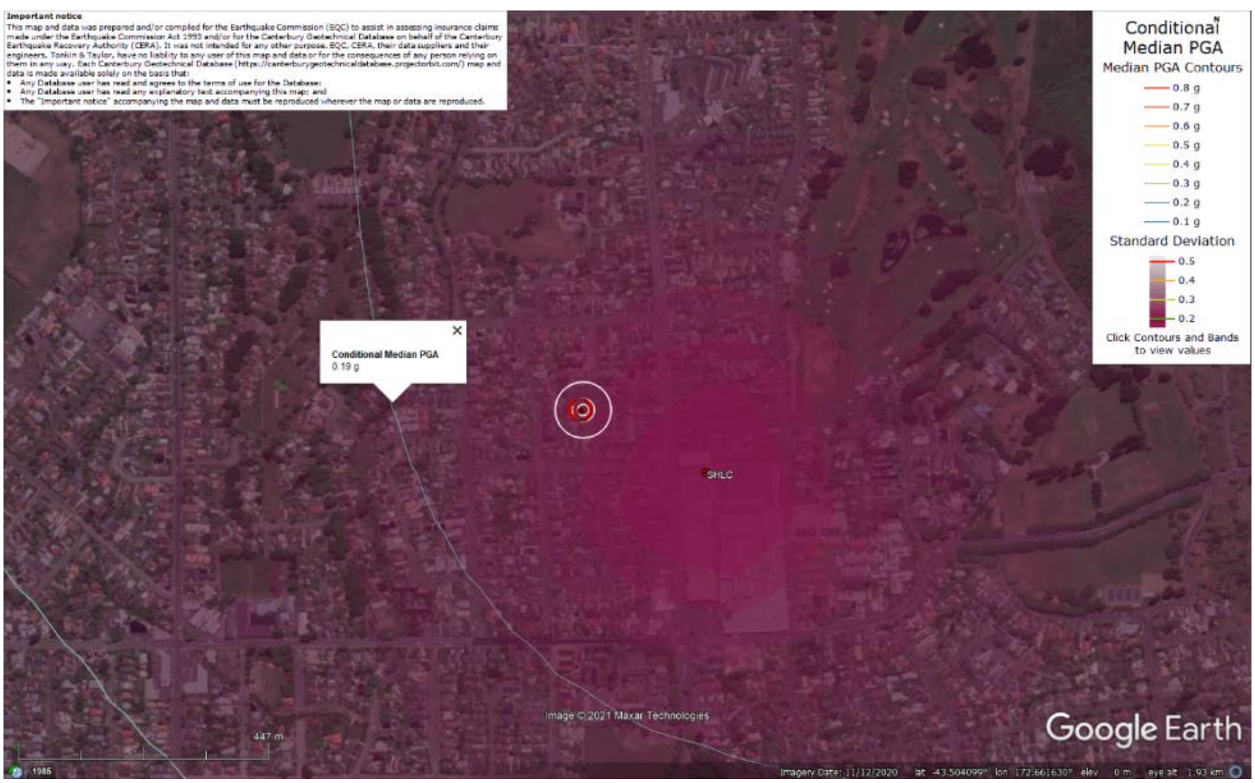

Figure 39: PGA for Sep-10 EQ (st. dev. = 0.175-0.225 ln units).

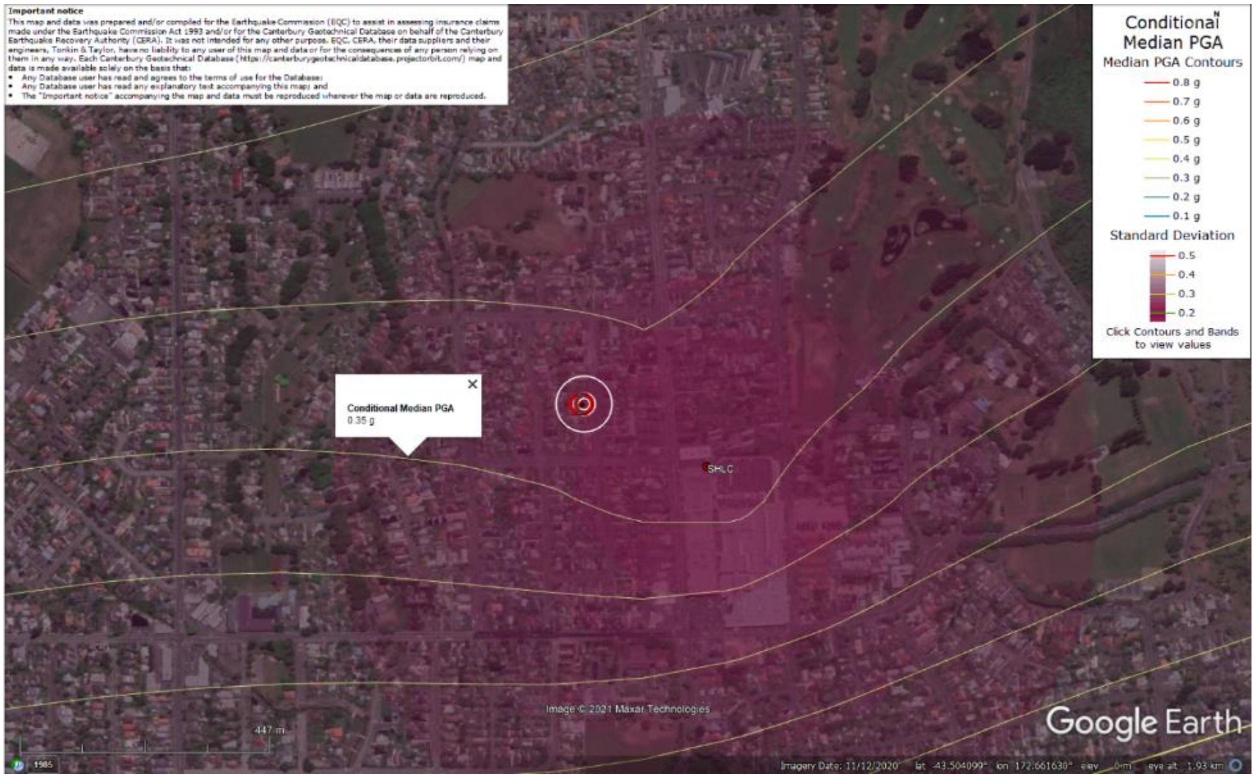

Figure 40: PGA for Feb-11 EQ (st. dev. = 0.200-0.250 ln units).

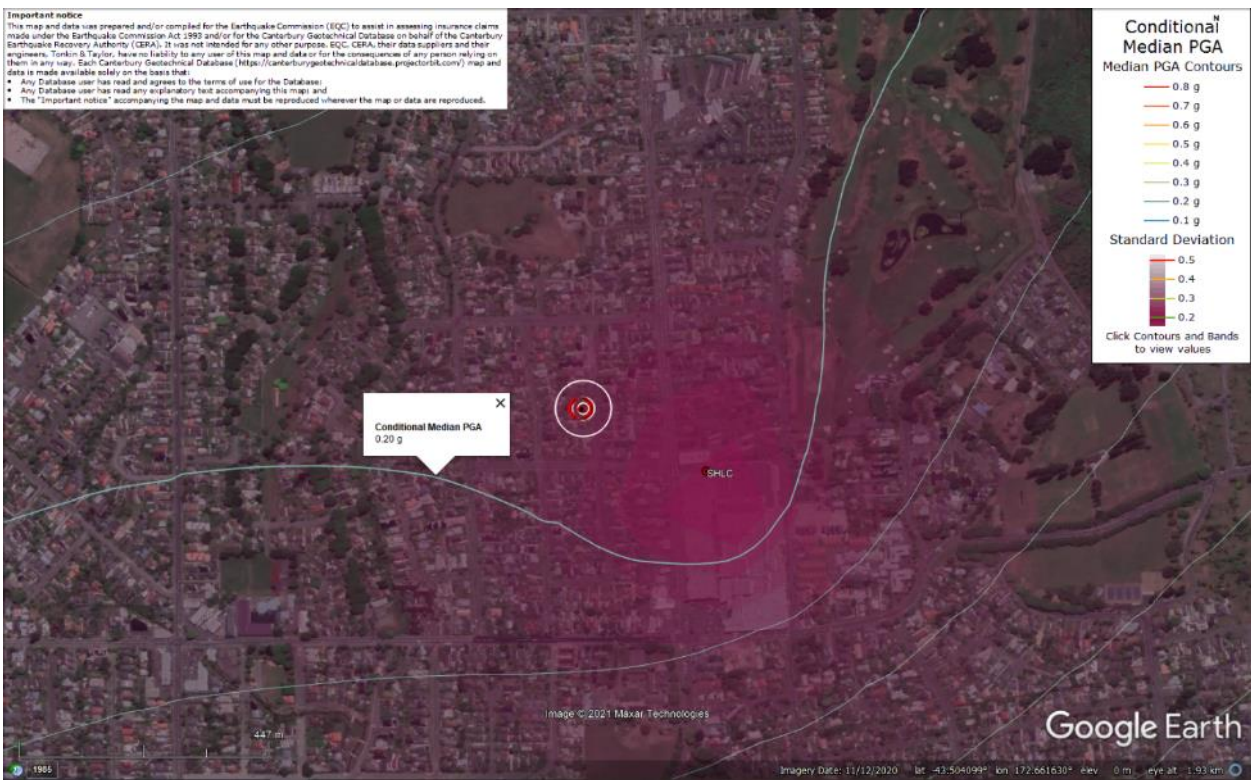

Figure 41: PGA for Jun-11 EQ (st. dev. = 0.225-0.250 ln units).

Figure 42: PGA for Dec-11 EQ (st. dev. = 0.225-0.250 ln units).

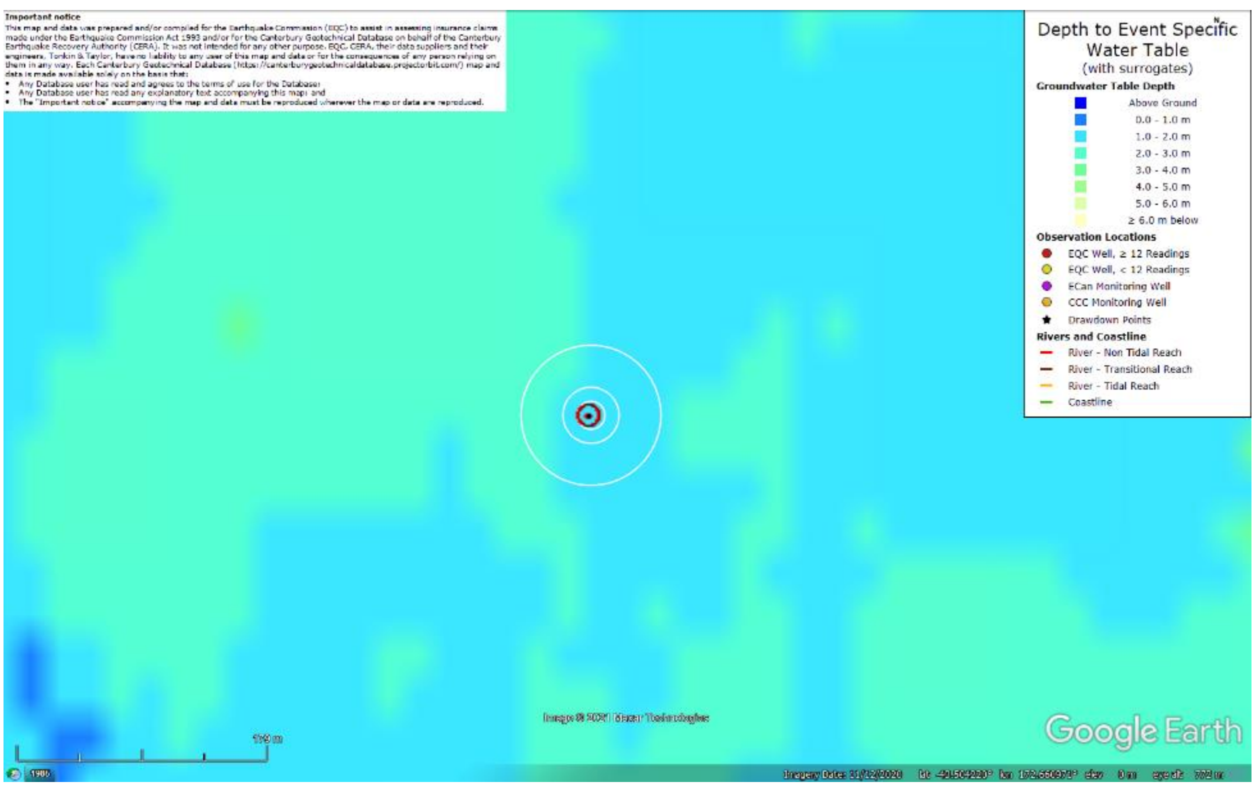

Figure 43: Depth to groundwater table for Sep-10 EQ.

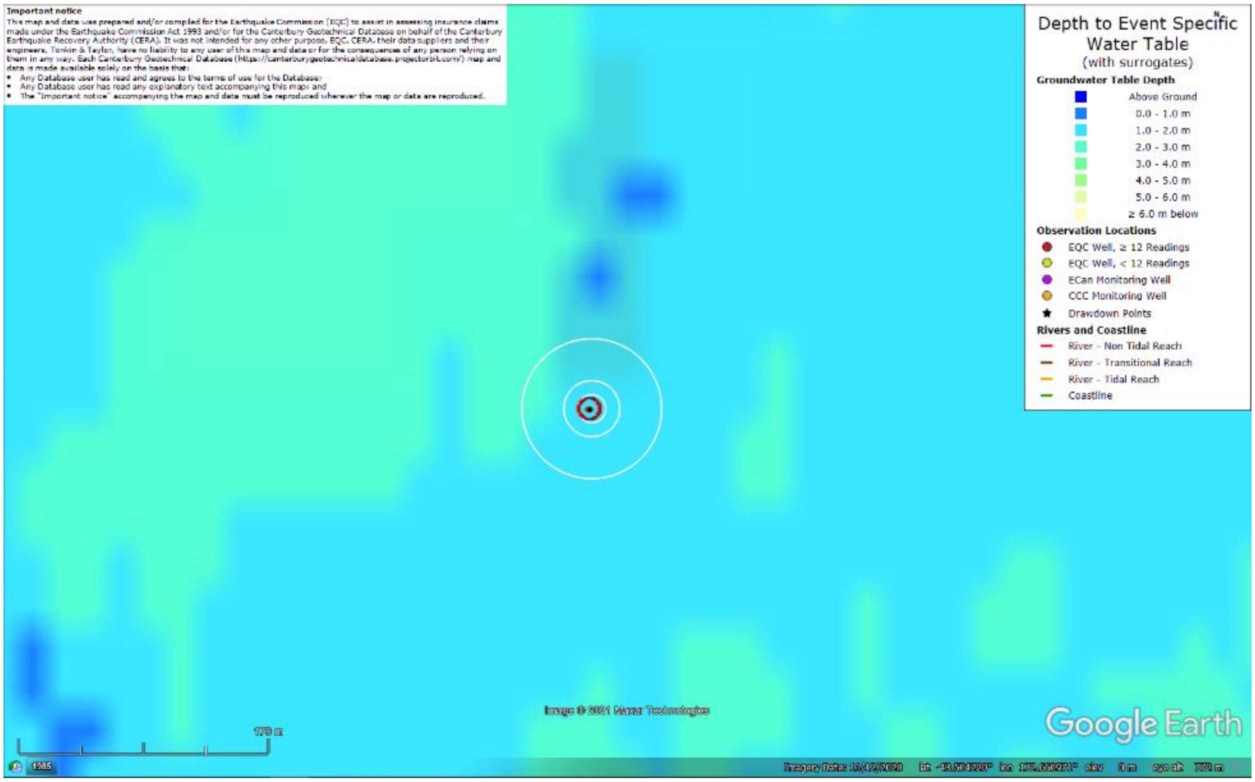

Figure 44: Depth to groundwater table for Feb-11 EQ.

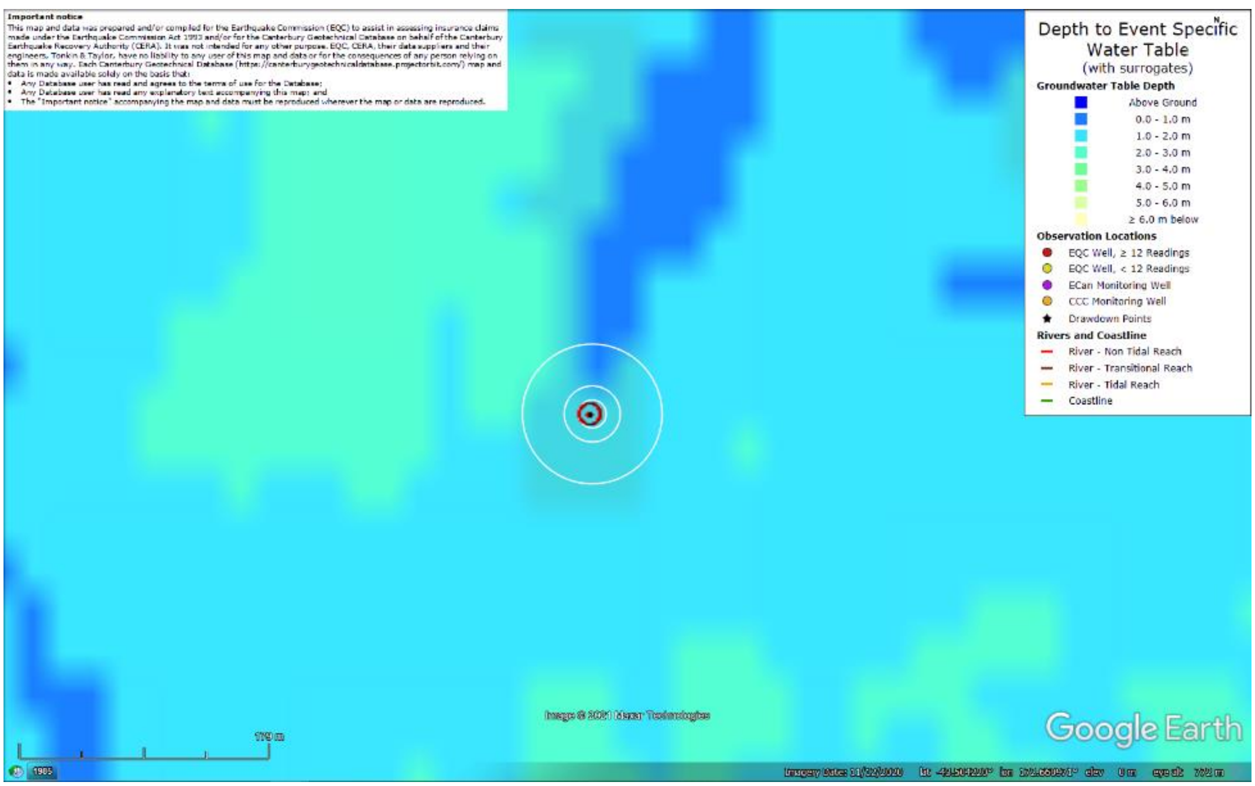

Figure 45: Depth to groundwater table for Jun-11 EQ.

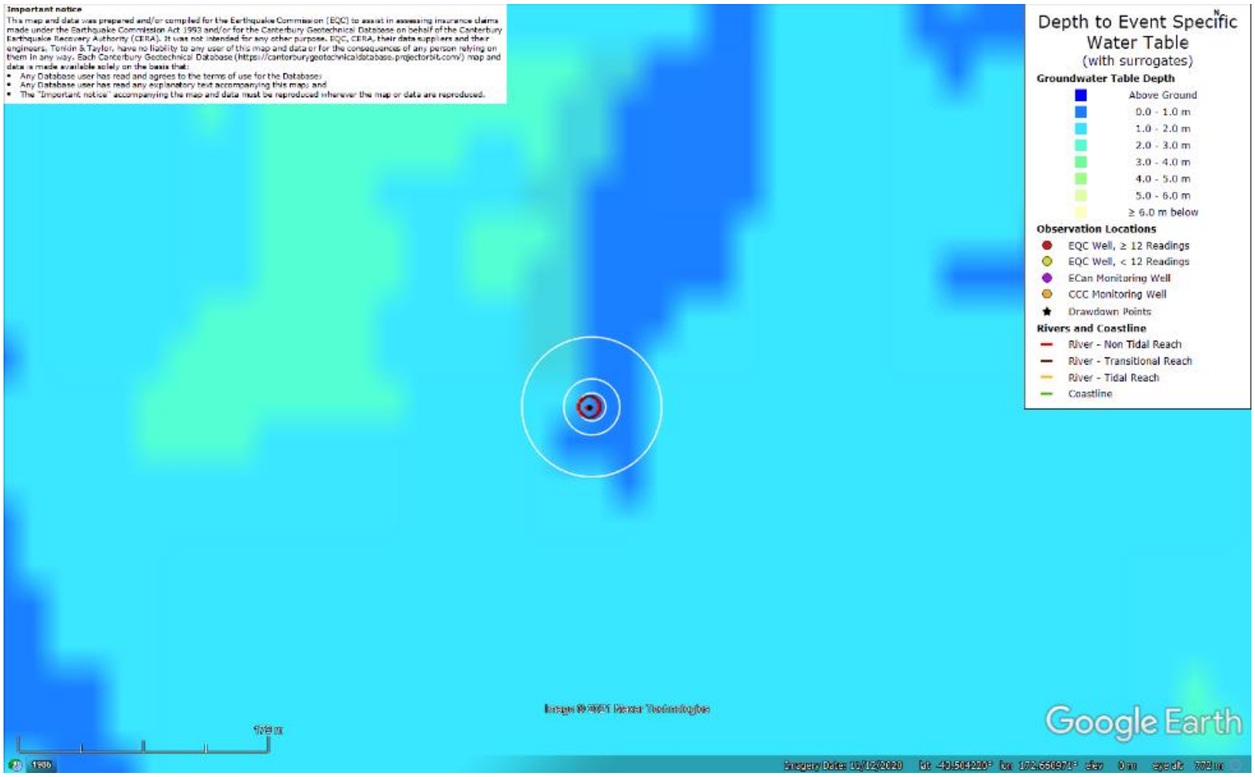

Figure 46: Depth to groundwater table for Dec-11 EQ.

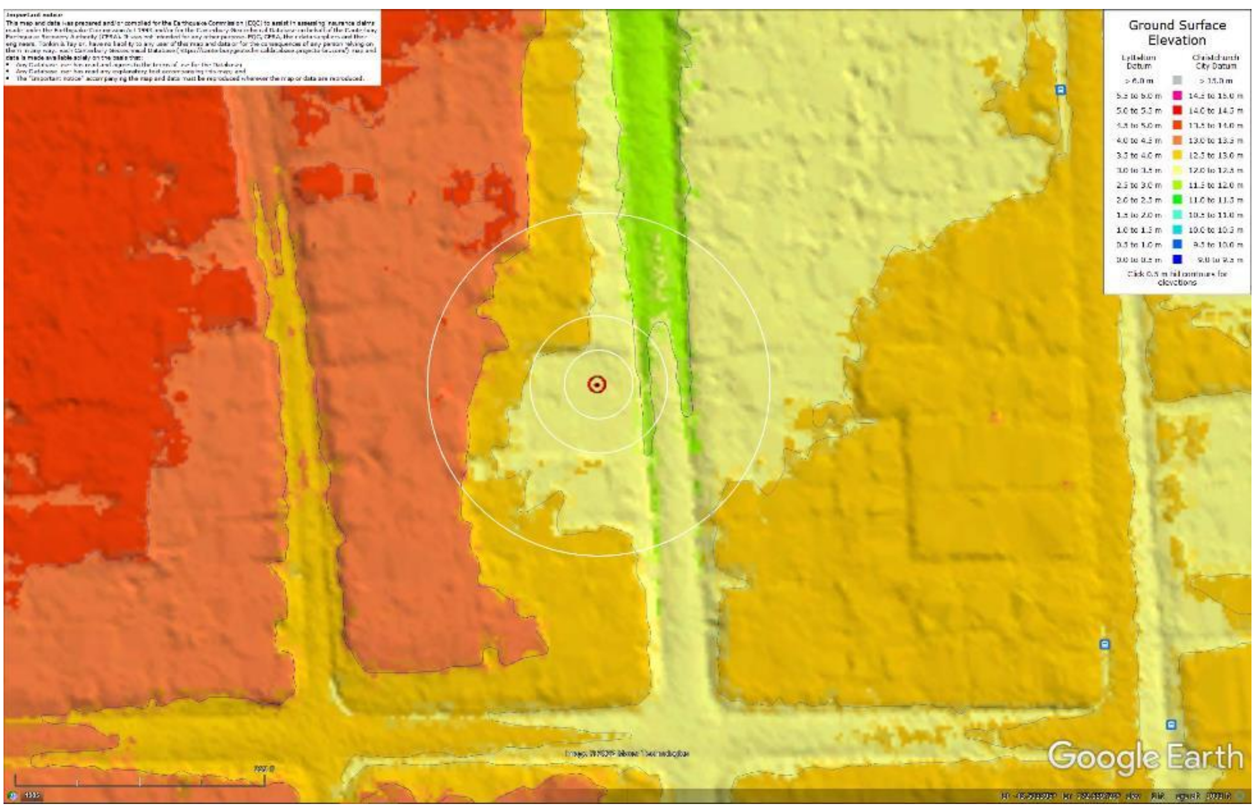

Figure 47: Ground surface elevation (Sep-11 LiDAR survey).

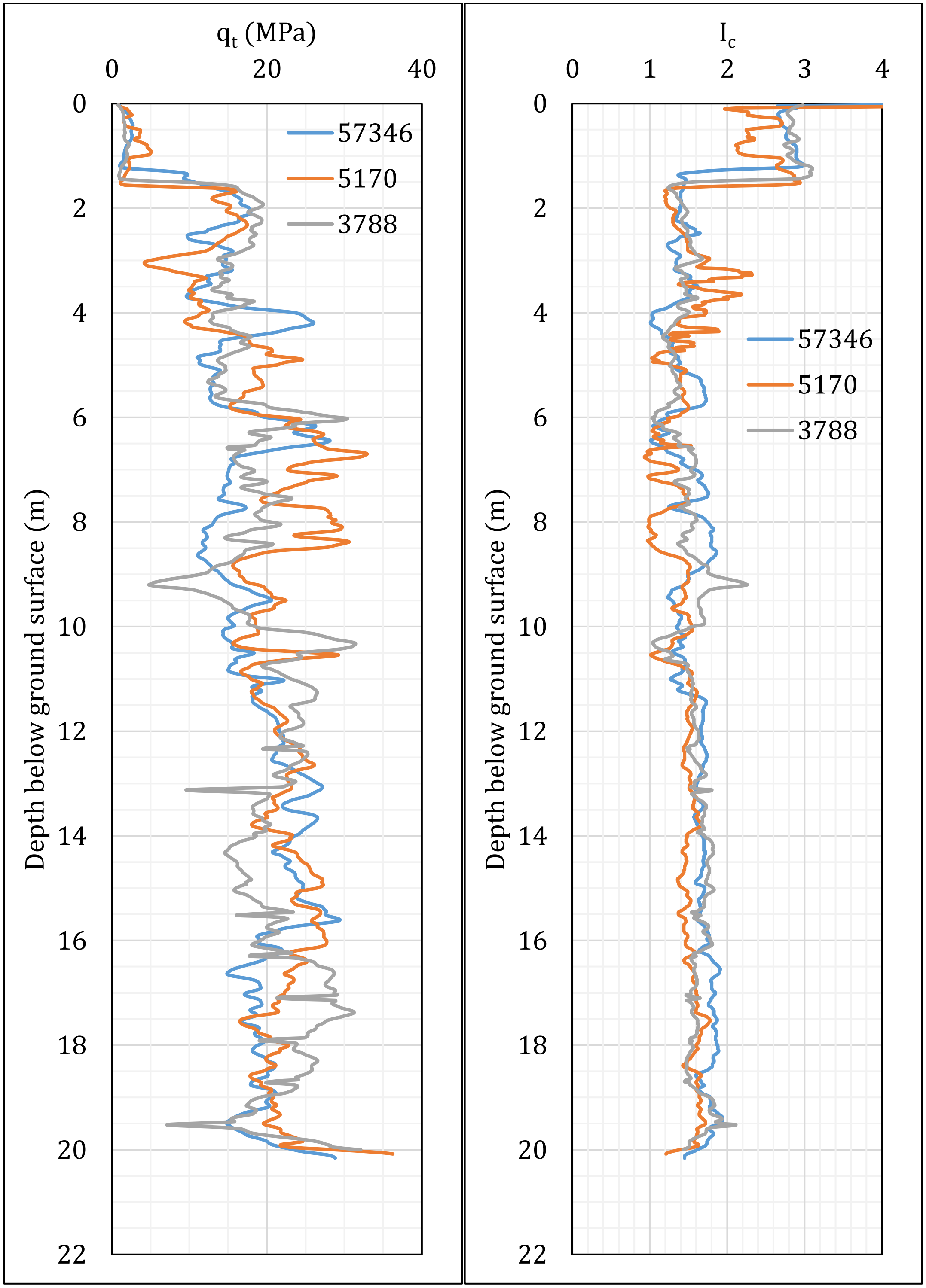

Figure 48: q_t and I_c profiles.

Note 5: The selection of CPTs for the area considered for settlement assessment (Figure 1) is based on the proximity of the CPTs to the considered areas. In accordance with that, the following table shows CPTs that were used for the volumetric settlement analysis in *Cliq v.3.0.3.2*, a CPT soil liquefaction software developed by GeoLogismiki. (The average volumetric settlements were reported in Table 8.)

Table 12: CPT profiles used in volumetric settlement analysis for areas selected for settlement assessment.

CPT ID No.	Patch A (10-m buffer)	Patch A (20-m buffer)	Patch A (50-m buffer)	Road
57346 (56586)	✓	✓	✓	✓
5170				✓
3788				✓

Table 13: CPT-based results.

		CPT ID		
EQ Event	Parameter	57346	5170	3788
Sep-10	S_{V1D} (mm)	0	3	4
	LSN	0	1	0
	LPI	0	0	0
	LPI_{ish}	0	0	0
	$D_{FS<1}$ (m)	undet.	undet.	undet.
Feb-11	S_{V1D} (mm)	3	7	12
	LSN	0	2	1
	LPI	0	1	1
	LPI_{ish}	0	1	0
	$D_{FS<1}$ (m)	undet.	2.92	9.08
Jun-11	S_{V1D} (mm)	0	4	3
	LSN	0	1	0
	LPI	0	0	0
	LPI_{ish}	0	0	0
	$D_{FS<1}$ (m)	undet.	undet.	undet.
Dec-11	S_{V1D} (mm)	1	7	8
	LSN	0	2	1
	LPI	0	1	0
	LPI_{ish}	0	1	0
	$D_{FS<1}$ (m)	undet.	undet.	undet.

Notes: $D_{FS<1}$ = Depth to the first liquefiable layer (FS_L<1) that is at least 200-mm thick, as determined by the Boulanger and Idriss (2016) liquefaction-triggering procedure (P_L=50%, C_{FC}=0.13, and $I_{c,cutoff}$ =2.6), and exported from *Cliq v.3.0.3.2*; undet. = the specified soil layer was not detected.

Note 6: Based on the borehole log (BH 57242, Figure 1), the groundwater table is at a depth of 1.6 m below the ground surface. The soil profile consists of (1) silt, ML, the Yaldhurst member of the Springston formation, to a depth of 1.2 m, (2) fine to medium sand, SP, the Yaldhurst member of the Springston formation, to a depth of 2.4 m, (3) sandy fine to coarse gravel, GW, the Yaldhurst member of the Springston formation, to a depth of 5.4 m, (4) fine to medium sand, SP, of the Christchurch formation to a depth of 5.8 m, (5) sandy fine to medium gravel, GW, of the Christchurch formation to a depth of 7.15, (6) fine to medium sand, SP, of the Christchurch formation to a depth of 9.1 m, (7) sandy fine to medium gravel, GW, of the Christchurch formation to a depth of 11.8 m, and (8) fine to medium sand, SP, of the Christchurch formation to a depth of 15.65 m (the end of the borehole).

Note 7: The ejecta-induced free-field settlement provided in Table 11 is an areal average settlement due to ejecta, which is based on the total settlement assessment area, A_T (provided in Table 9 and repeated in Table 14). However, the considered area was not always covered completely with ejecta; thus, it is important to provide the localized ejecta-induced settlement, too. The localized settlement due to ejecta is estimated using photographic evidence only as

$$S_{E,P\_localized} = \frac{V_E}{A_E}$$

where V_E is the total volume of ejecta within A_T and A_E is the total coverage area of ejecta within A_T. Please note that the areal ejecta-induced settlement provided in Table 14 as S_{E,P_areal} is the same as $S_{E,P}$ in Table 11, which was estimated as

$$S_{E,P\_areal} = S_{E,P} = \frac{V_E}{A_T}$$

where V_E is the total volume of ejecta within A_T and A_T is the total settlement assessment area.

Table 14a: Areal and localized ejecta-induced settlement estimates for Patch A (10-m buffer) based on photographic evidence.

Earthquake Event	A_T (m^2)	A_E (m^2)	V_E (m^3)	S_{E,P_areal} (mm)	$S_{E,P\_localized}$ (mm)
Sep-10	296	0	0	0	0
Feb-11	296	141	2.8-5.0	15±5	30±5
Jun-11	296	192	3.8-5.8	15±5	25±5
Dec-11	288	3.9	0.04-0.08	<5	15±5

Notes: S_{E,P_areal} = $S_{E,P}$ reported in Table 11 = areal ejecta-induced settlement; $S_{E,P\_localized}$ = localized ejecta-induced settlement; A_T = total settlement assessment area; V_E = total volume of ejecta within A_T; A_E = total area of ejecta within A_T; The estimates of both areal and localized ejecta-induced settlement are rounded to the nearest 5; Final plus/minus values are also rounded to the nearest 5.

Table 14b: Areal and localized ejecta-induced settlement estimates for Patch A (20-m buffer) based on photographic evidence.

Earthquake Event	A_T (m^2)	A_E (m^2)	V_E (m^3)	S_{E,P_areal} (mm)	$S_{E,P\_localized}$ (mm)
Sep-10	710	0	0	0	0
Feb-11	710	229	5.8-10.6	10±5	35±10
Jun-11	710	342	6.8-10.3	15±5	25±5
Dec-11	701	11.6	0.1-0.3	<5	20±5

Notes: S_{E,P_areal} = $S_{E,P}$ reported in Table 11 = areal ejecta-induced settlement; $S_{E,P\_localized}$ = localized ejecta-induced settlement; A_T = total settlement assessment area; V_E = total volume of ejecta within A_T; A_E = total area of ejecta within A_T; The estimates of both areal and localized ejecta-induced settlement are rounded to the nearest 5; Final plus/minus values are also rounded to the nearest 5.

Table 14c: Areal and localized ejecta-induced settlement estimates for Patch A (50-m buffer) based on photographic evidence.

Earthquake Event	A_T (m^2)	A_E (m^2)	V_E (m^3)	S_{E,P_areal} (mm)	$S_{E,P\_localized}$ (mm)
Sep-10	885	0	0	0	0
Feb-11	885	339	11.9-21.7	20±5	50±15
Jun-11	885	347	6.9-10.4	10±5	25±5
Dec-11	860	23.5	0.4-0.9	<5	30±10

Notes: S_{E,P_areal} = $S_{E,P}$ reported in Table 11 = areal ejecta-induced settlement; $S_{E,P\_localized}$ = localized ejecta-induced settlement; A_T = total settlement assessment area; V_E = total volume of ejecta within A_T; A_E = total area of ejecta within A_T; The estimates of both areal and localized ejecta-induced settlement are rounded to the nearest 5; Final plus/minus values are also rounded to the nearest 5.

Table 14d: Areal and localized ejecta-induced settlement estimates for Road (50-m buffer) based on photographic evidence.

Earthquake Event	A_T (m^2)	A_E (m^2)	V_E (m^3)	S_{E,P_areal} (mm)	$S_{E,P\_localized}$ (mm)
Sep-10	1297	0	0	0	0
Feb-11	1297	1297	51.0-83.4	50±10	50±10
Jun-11	1225	1225	27.7-50.3	30±10	30±10
Dec-11	1282	137	3.5-4.9	5±5	30±5

Notes: S_{E,P_areal} = $S_{E,P}$ reported in Table 11 = areal ejecta-induced settlement; $S_{E,P\_localized}$ = localized ejecta-induced settlement; A_T = total settlement assessment area; V_E = total volume of ejecta within A_T; A_E = total area of ejecta within A_T; The estimates of both areal and localized ejecta-induced settlement are rounded to the nearest 5; Final plus/minus values are also rounded to the nearest 5.

Summary 2:

- **The best estimate of the localized ejecta-induced free-field ground settlement at the Sabina Playground site for the SEP 2010, FEB 2011, JUN 2011, and DEC 2011 earthquake is 0 mm, 50±15 mm, 25±5 mm, and 30±10 mm, respectively.**

- **The best estimate of the localized ejecta-induced settlement of the road at the Sabina Playground site for the SEP 2010, FEB 2011, JUN 2011, and DEC 2011 earthquake is 0 mm, 50±10 mm, 30±10 mm, and 30±5 mm, respectively.**